

Light-Front Dynamics in Hadron Physics

Chueng-Ryong Ji
North Carolina State University



Inha HTG workshop: Modern issues in Hadronic Physics

July 7, 2022

Outline

- QCD Local and Global Symmetries
- Color Confinement and Chiral Symmetry
- Dirac's Proposition for Relativistic Dynamics
- Distinguished Features of Light-Front Dynamics
- Large N_c QCD in 1+1 dim. ('tHooft Model)
- Application to Hadron Phenomenology

Quantum Chromodynamics (QCD)

$$\mathcal{L}_{\text{QCD}} = \sum_{i,j=1}^3 \bar{q}_i (i \not{D} - m_q)_{ij} q_j - \frac{1}{4} \sum_{\alpha=1}^8 G_{\mu\nu}^{\alpha} G^{\alpha,\mu\nu}$$

Local $SU(3)_c$ Gauge Theory

interrelated with

Global Symmetry

Isospin symmetry

Chiral symmetry

$SU(2)_R \times SU(2)_L$

Spontaneous symmetry breakdown

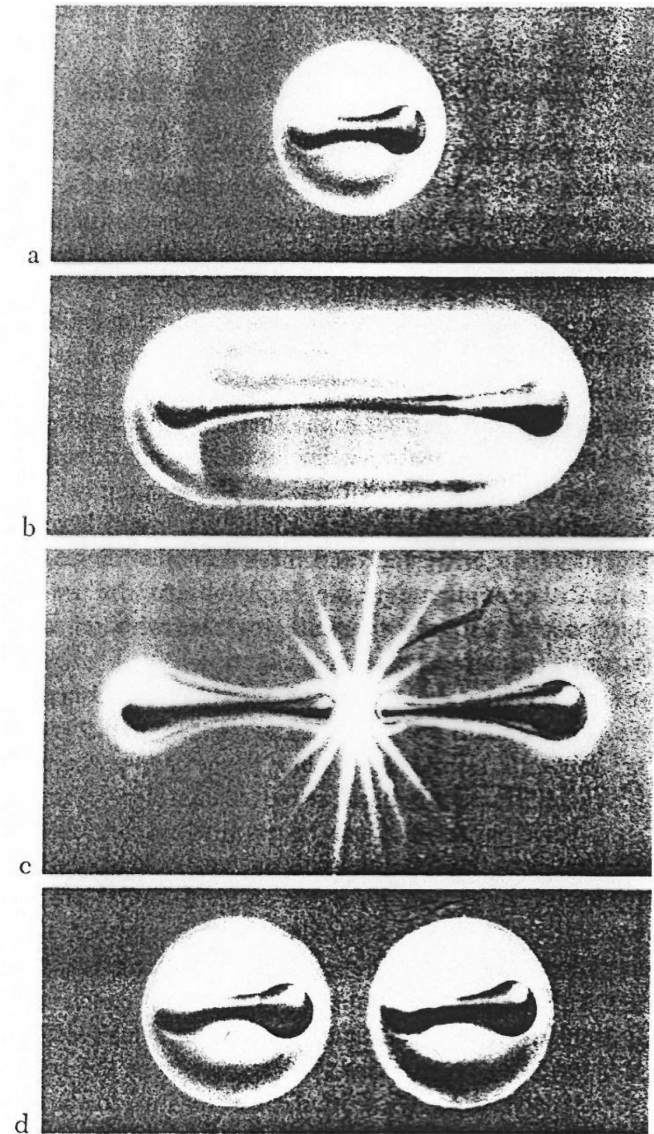
Goldstone Bosons

$$F_{\pi}^2 M_{\pi}^2 = -(m_u + m_d) \langle 0 | \bar{u}u | 0 \rangle$$

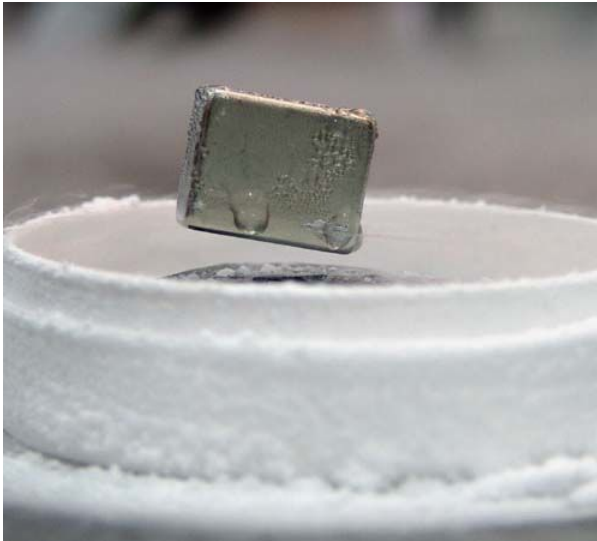
Effective field theory

Confinement and Vacuum Condensation are intimately linked to each other.

Vacuum Condensation indicates that the vacuum symmetry is Broken due to the condensation.

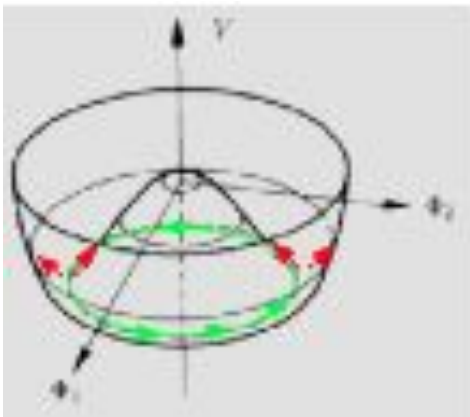


Meissner Effect of Superconductor



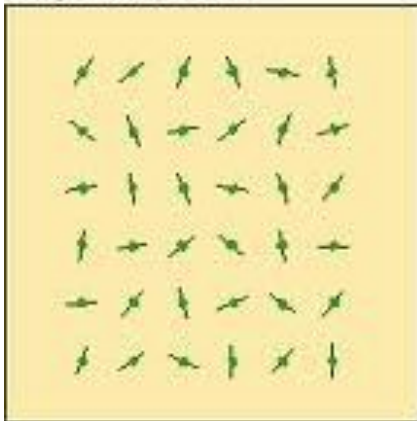
$$m\dot{\vec{x}} = \vec{p} - e\vec{A}$$

$$D_\mu\phi = \partial_\mu\phi - eA_\mu\phi$$

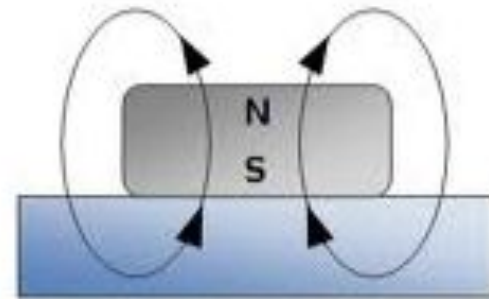
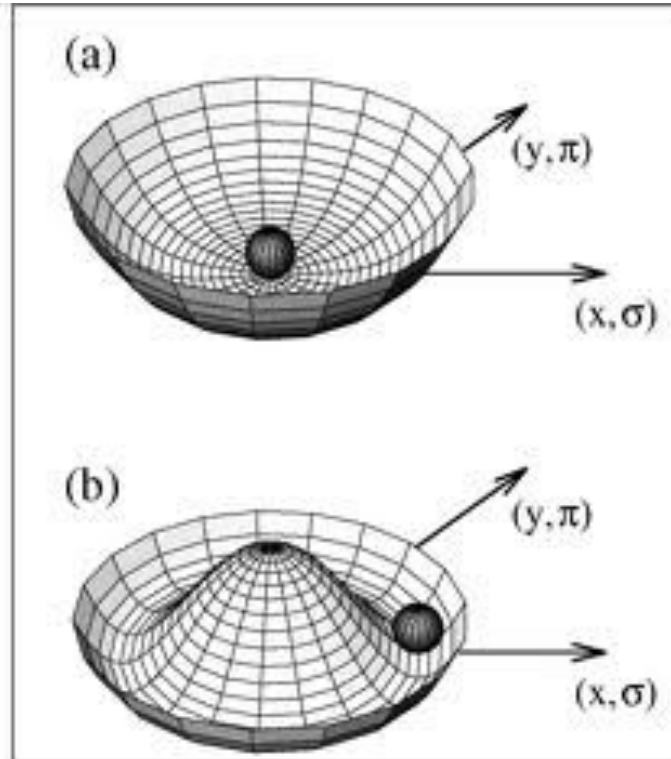


$$\phi = \begin{pmatrix} 0 \\ V + \eta \end{pmatrix} \Rightarrow m_\eta = \sqrt{\lambda V}, m_W = gV, \dots$$

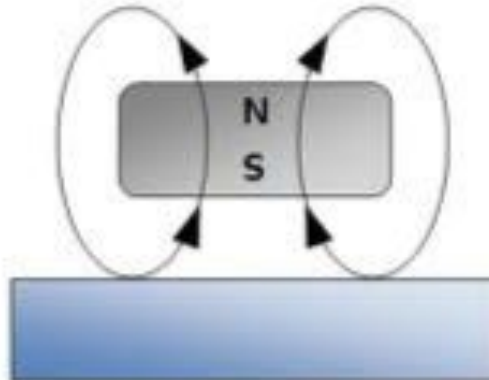
High Temperature



Low Temperature

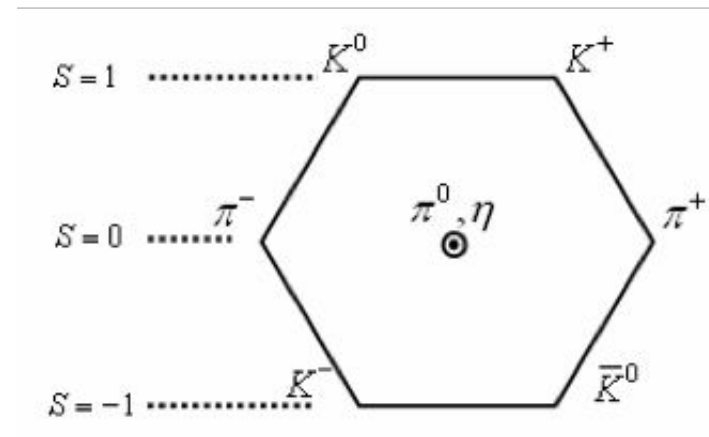
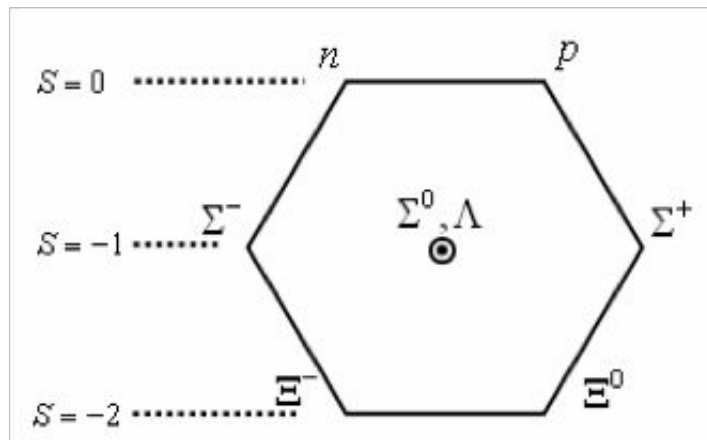


Superconductor:
Above Critical Temp.



Superconductor:
Below Critical Temp.

Chiral symmetry breaking in QCD vacuum

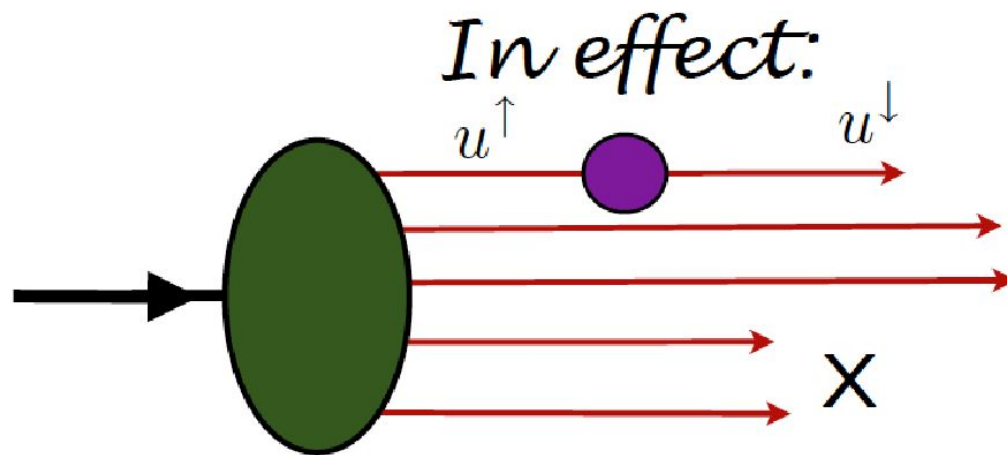
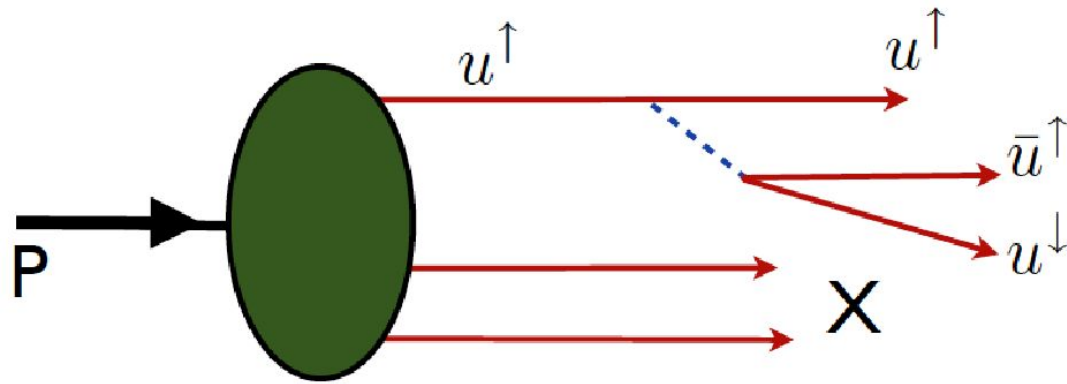


No parity doubled baryons

Pseudo Goldstone meson

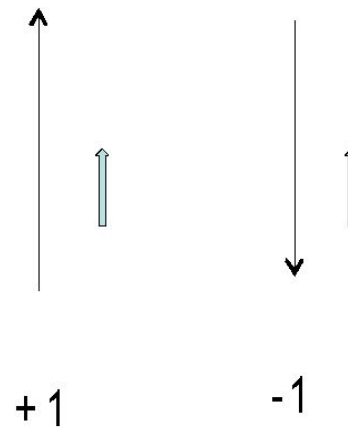
Low energy PCAC phenomenology and Chiral effective theory

Chiral Symmetry in QCD



Consistency with Relativistic Dynamics

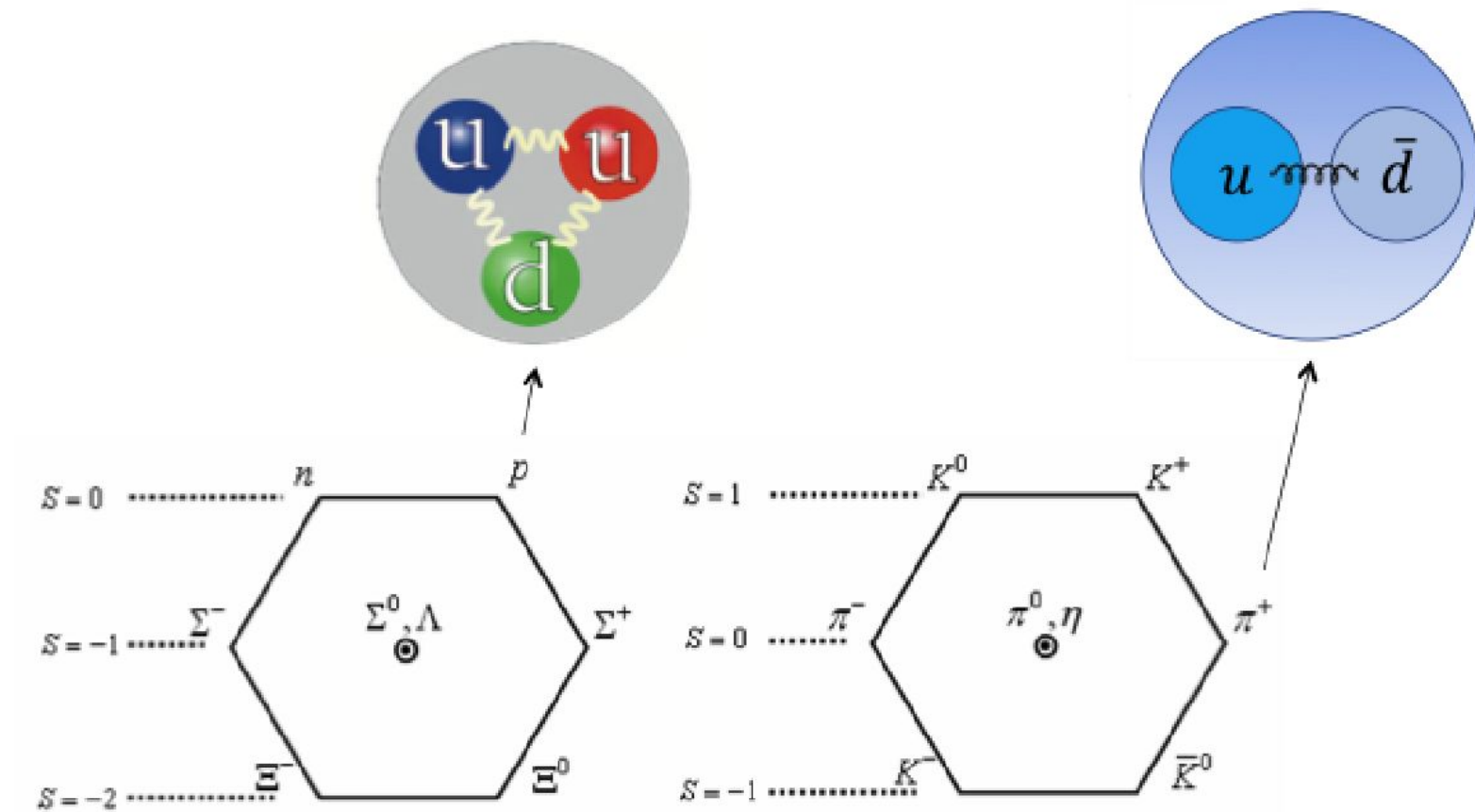
Helicity is invariant for $m=0$



Helicity = Chirality for $m=0$

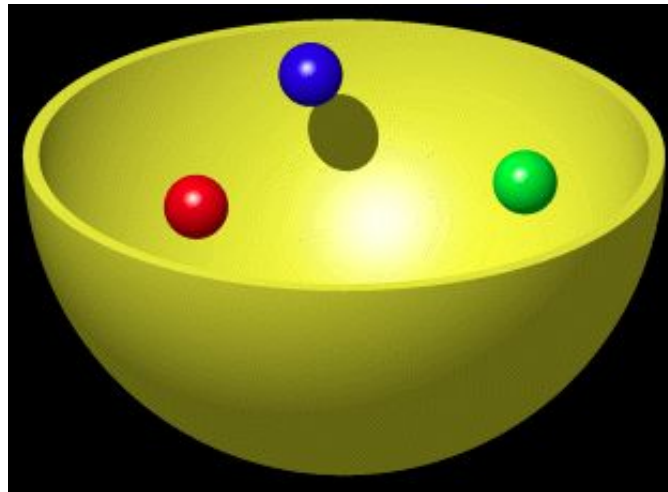
Chiral Symmetry Breaking due to
dynamical mass generation

How do we understand the Quark Model in Quantum Chromodynamics?



$$M_p = 938.272046 \pm 0.000021 \text{ MeV}$$

$$M_n = 939.565379 \pm 0.000021 \text{ MeV}$$

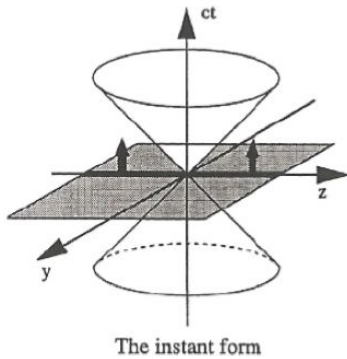


$$m_u = 2.3_{-0.5}^{+0.7} \text{ MeV} \quad ; \quad m_d = 4.8_{-0.3}^{+0.7} \text{ MeV}$$

Dirac's Proposition for Relativistic Dynamics



1949

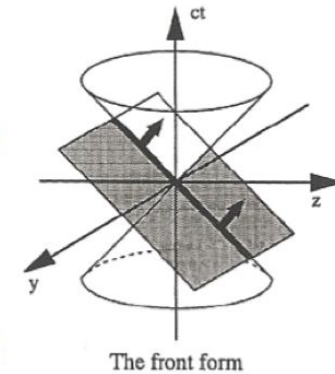


Equal t

$$p^0 \Leftrightarrow (p^1, p^2) \Leftrightarrow p^3$$

Equal τ

$$p^- = p^0 - p^3 \Leftrightarrow \vec{p}_\perp \Leftrightarrow p^+ = p^0 + p^3$$



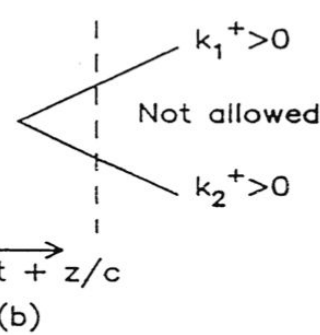
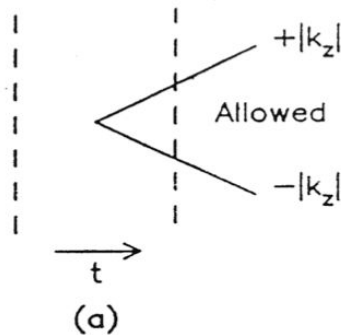
Energy-Momentum Dispersion Relations

$$p^0 = \sqrt{\vec{p}^2 + m^2}$$

$$p^- = \frac{\vec{p}_\perp^2 + m^2}{p^+}$$

IFD

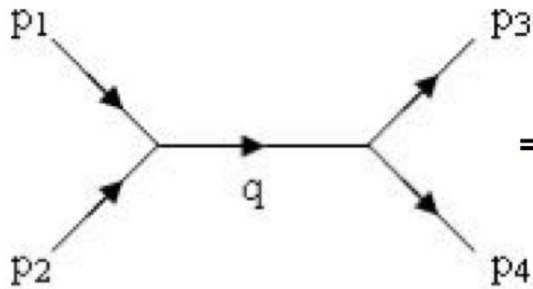
Instant Form Dynamics



LFD

Light-Front Dynamics

$$"e^+ e^- \rightarrow \mu^+ \mu^-"$$



$$= \frac{1}{q^2 - m^2} = \frac{1}{s - m^2} \quad q^2 = (p_1 + p_2)^2 \neq m^2$$

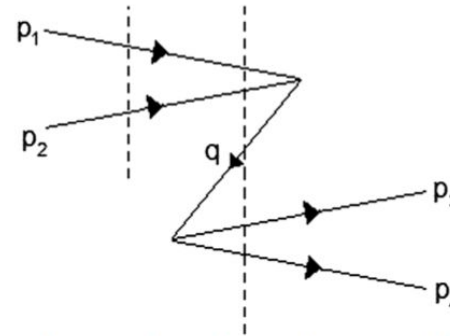
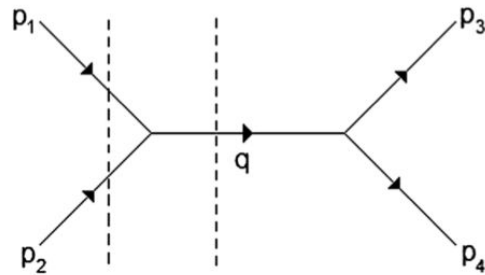
Four-momentum conservation but off-mass-shell

Feynman Diagram: Invariant under all 10 Poincaré generators

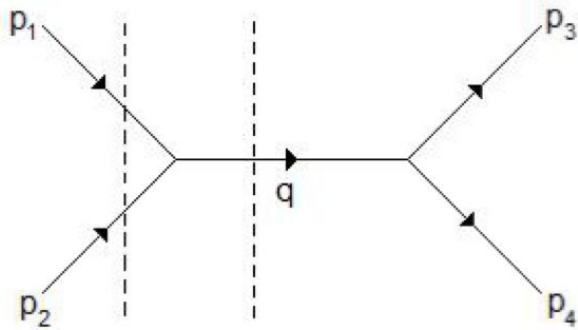
$t \rightarrow$ (time evolution; time ordered process in QFT; Energy is not conserved within Δt)

$$(\Delta E)(\Delta t) \sim \hbar$$

Three-momentum conservation but on-mass-shell

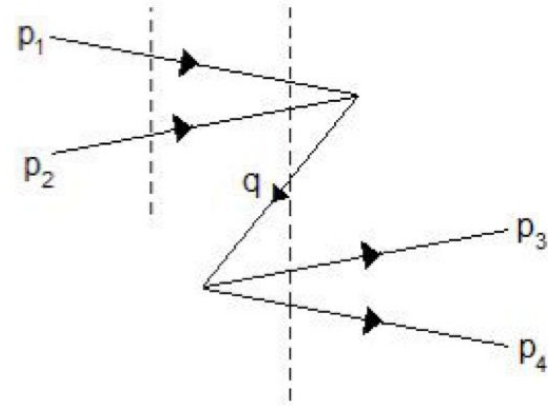


Individual Time-Ordered Diagrams: Invariant only under translation and rotation (6 kinematic generators)



(a)

$$\Sigma_{\text{IFD}}^a = \frac{1}{2q^0} \left(\frac{1}{p_1^0 + p_2^0 - q^0} \right)$$



(b)

$$\Sigma_{\text{IFD}}^b = -\frac{1}{2q^0} \left(\frac{1}{p_1^0 + p_2^0 + q^0} \right)$$

$$\Sigma_{\text{IFD}}^a + \Sigma_{\text{IFD}}^b = \frac{1}{2q^0} \left(\frac{1}{p_1^0 + p_2^0 - q^0} - \frac{1}{p_1^0 + p_2^0 + q^0} \right)$$

$$= \frac{1}{(p_1^0 + p_2^0)^2 - (q^0)^2}$$

$$= \frac{1}{\{(p_1^0 + p_2^0)^2 - (\vec{p}_1 + \vec{p}_2)^2\} - \{(q^0)^2 - \vec{q}^2\}}$$

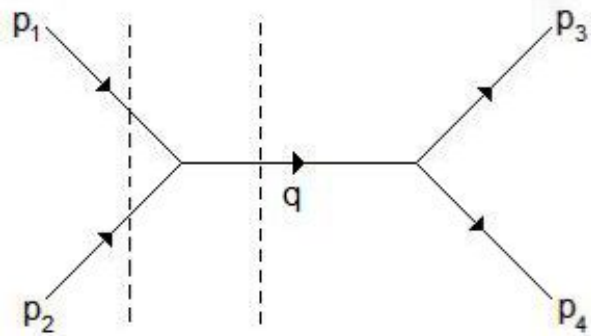
: Three-momentum conservation

$$= \frac{1}{(p_1 + p_2)^2 - q^2}$$

: $q^2 = m^2$; on-mass-shell

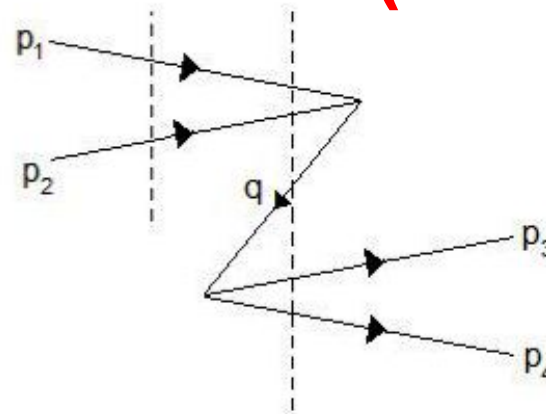
$$= \frac{1}{s - m^2}$$

Infinite Momentum Frame (IMF) Approach



(a)

$$\frac{1}{E_1 + E_2 - Eq}$$



(b)

$$\begin{aligned} & -\frac{1}{Eq + E_3 + E_4} \\ & = -\frac{1}{Eq + E_1 + E_2} \\ & \rightarrow 0 \end{aligned}$$

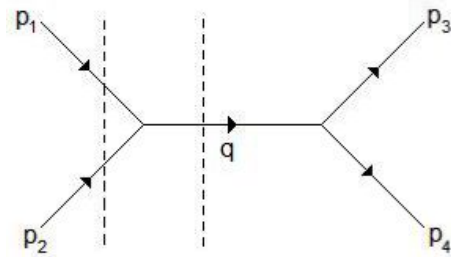
S.Weinberg, PR158,1638(1967)

“Dynamics at Infinite Momentum”

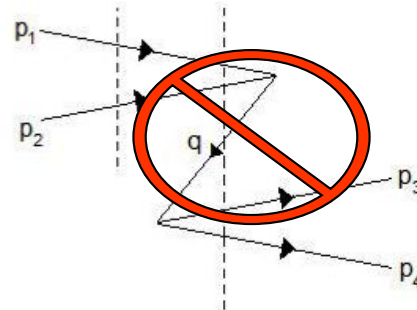
Note that this is still in the instant form (IFD).

However, in LFD, (b) drops for any reference frame (not just for IMF)

$\tau (= t+z/c) \rightarrow$



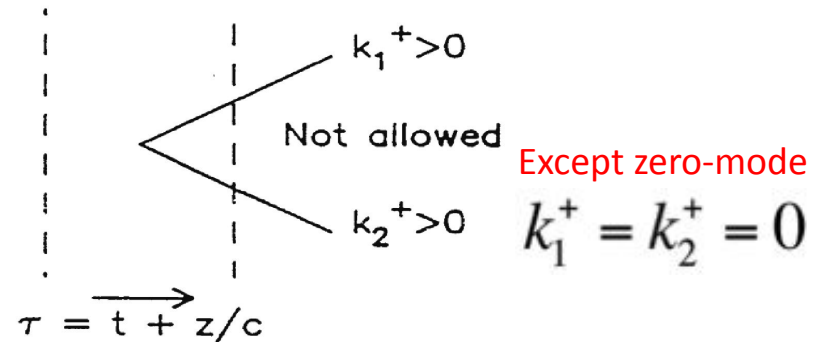
(a)



(b)

$$\begin{aligned} \Sigma_{LFD}^a + \Sigma_{LFD}^b &= \frac{1}{q^+} \left(\frac{1}{p_1^- + p_2^- - q^-} + 0 \right) \\ &= \frac{1}{q^+ \left(\frac{(p_1 + p_2)^2 + (\vec{p}_{1\perp} + \vec{p}_{2\perp})^2}{(p_1 + p_2)^+} - \frac{m^2 + \vec{q}_\perp^2}{q^+} \right)} \\ &= \frac{1}{(p_1 + p_2)^2 - m^2} \\ &= \frac{1}{s - m^2} \end{aligned}$$

$$p^- = \frac{\vec{p}_\perp^2 + m^2}{p^+}$$



QED Example

Anomalous Magnetic Moment

- Magnetic moment of a particle is related to its spin.

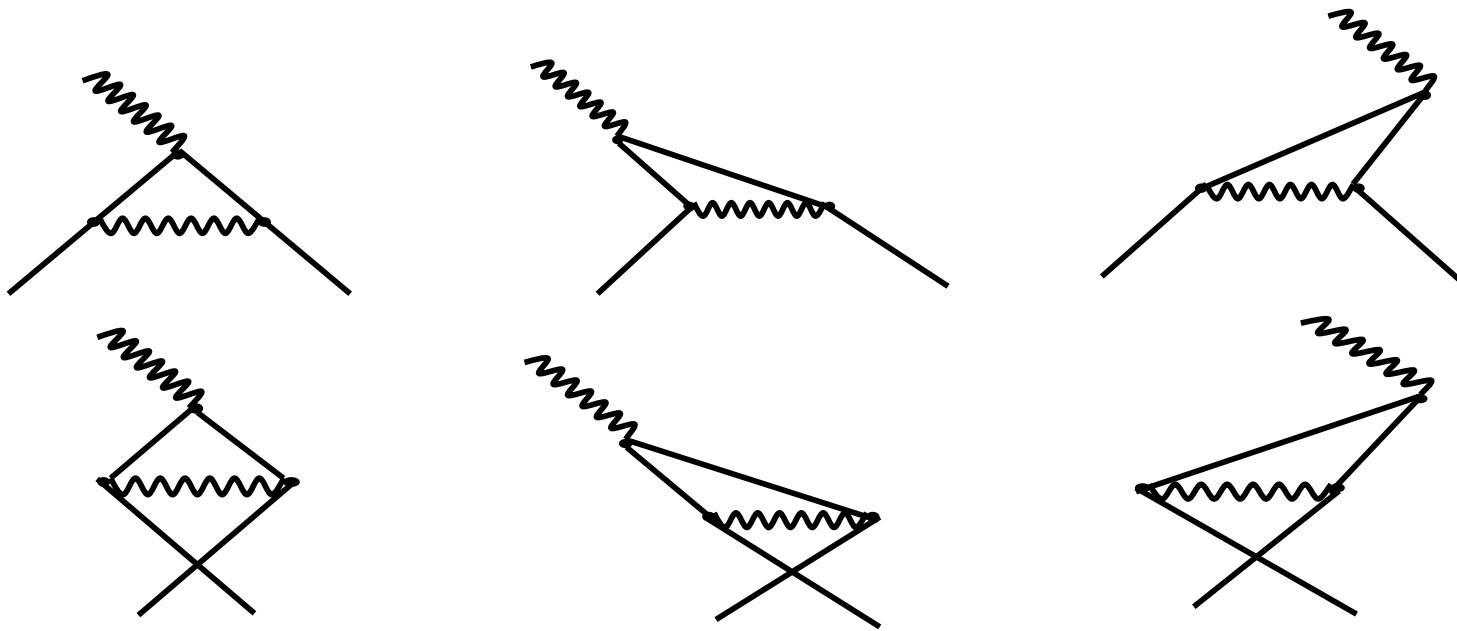
$$\vec{\mu} = g \frac{e\hbar}{2mc} \vec{S}$$

- For Dirac pointlike particle, $g=2$. However, the loop correction in QFT yields the non-zero $g-2$, i.e. anomalous magnetic moment.

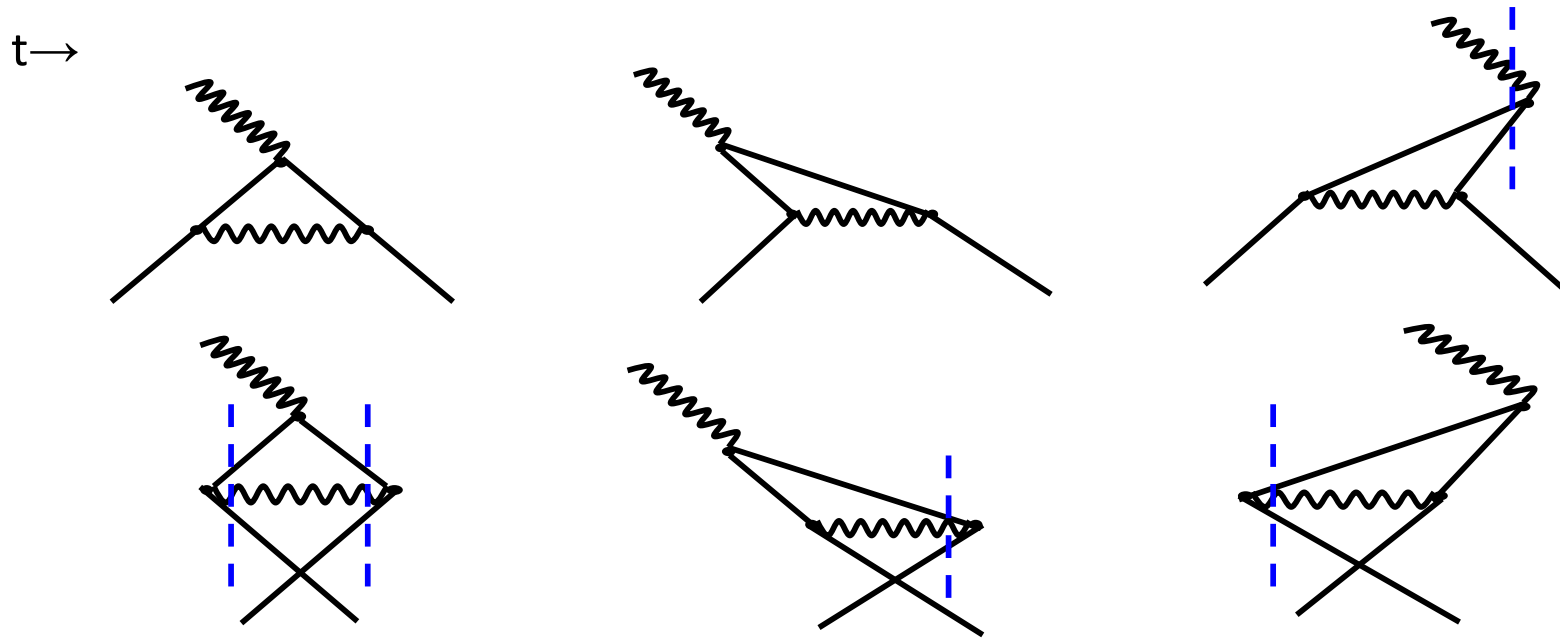


g-2 calculation

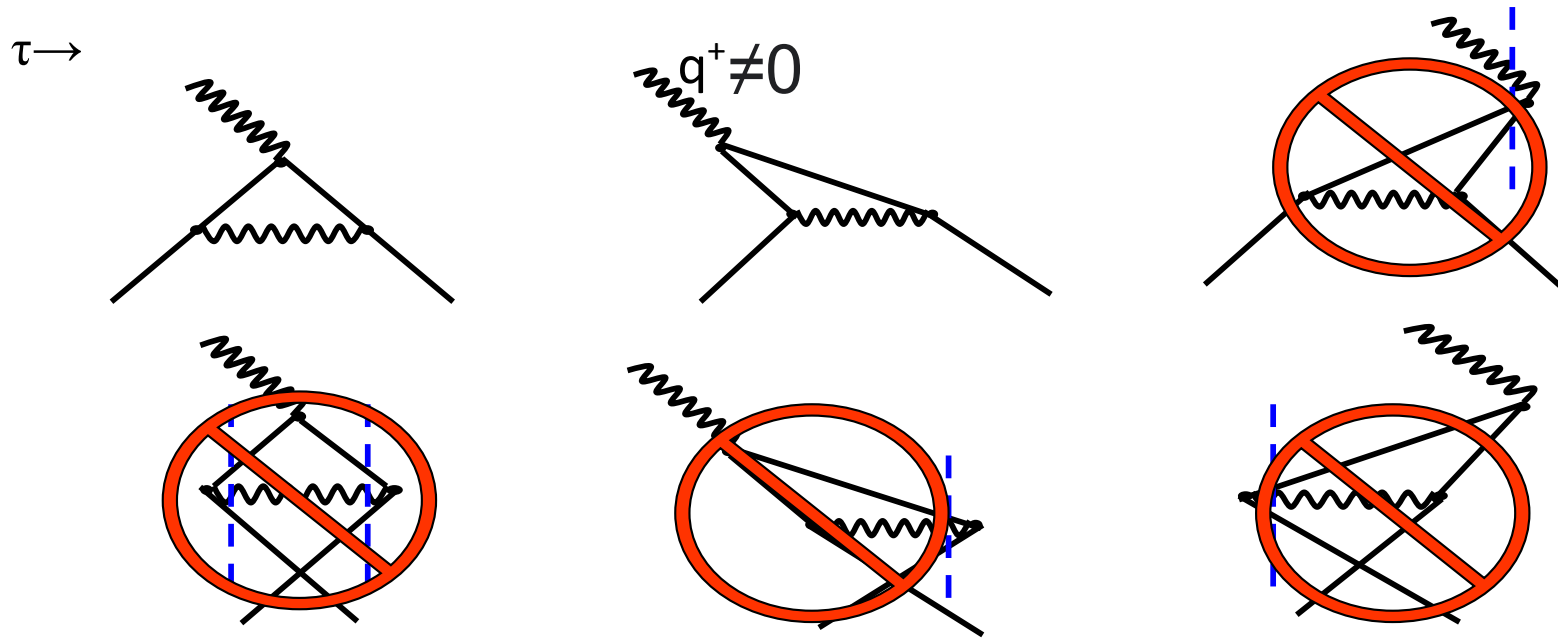
t →



g-2 calculation

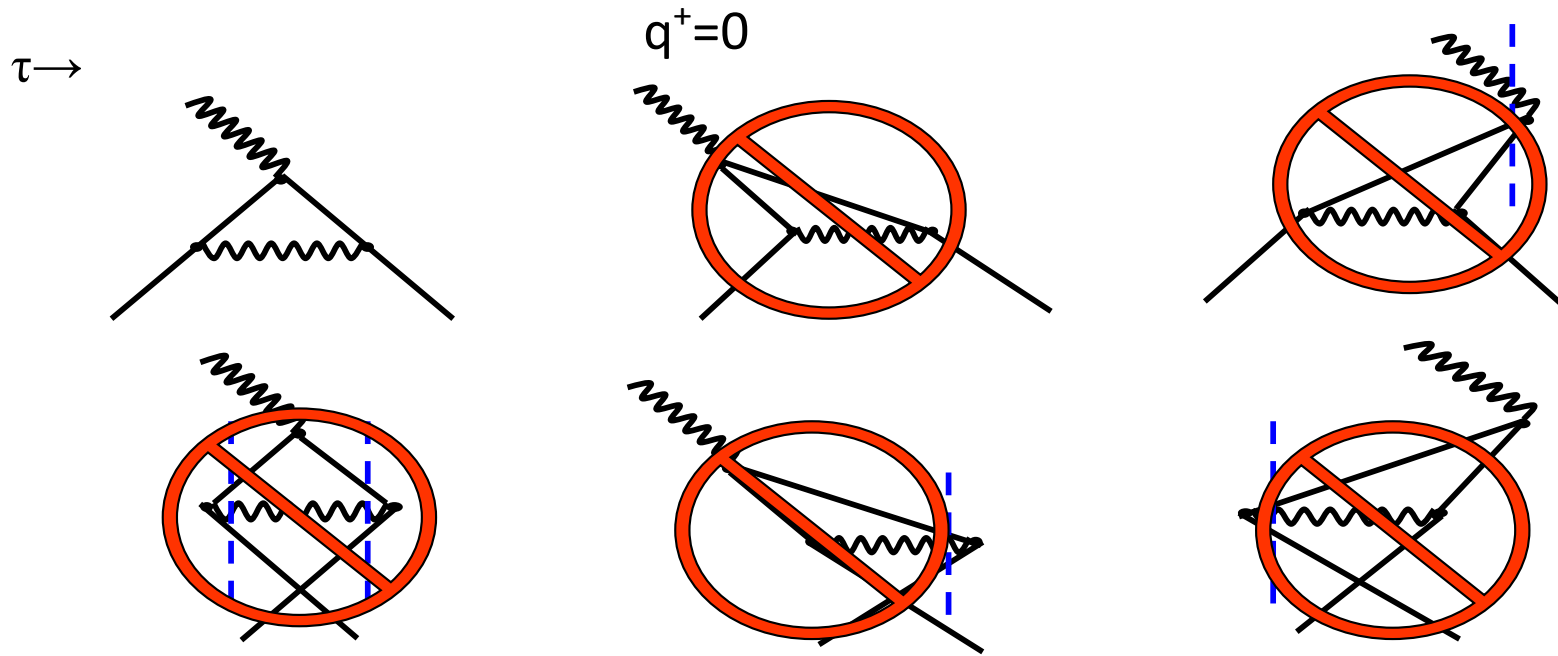


g-2 calculation



- Vacuum fluctuations are suppressed in LFD and clean hadron phenomenology is possible.

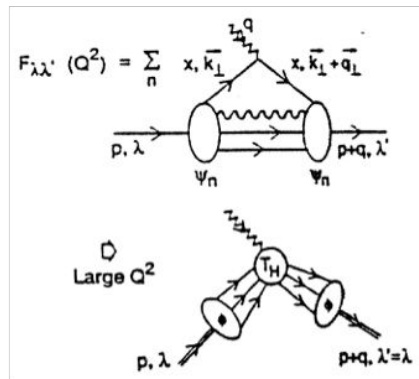
g-2 calculation



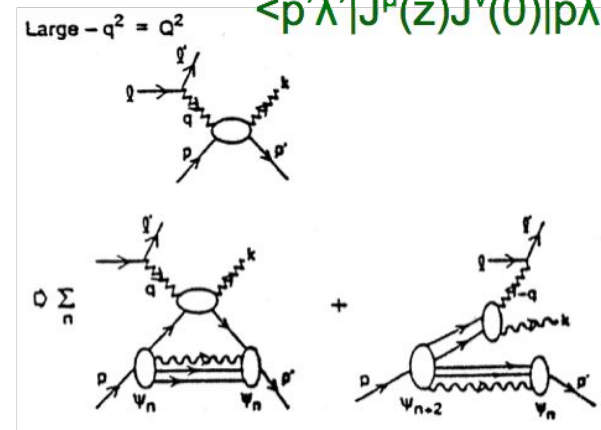
- Vacuum fluctuations are suppressed in LFD and clean hadron phenomenology is possible. **Note that the dynamical difference between $q^+ = 0$ and $q^+ \neq 0$.**

Applications to Hadron Phenomenology

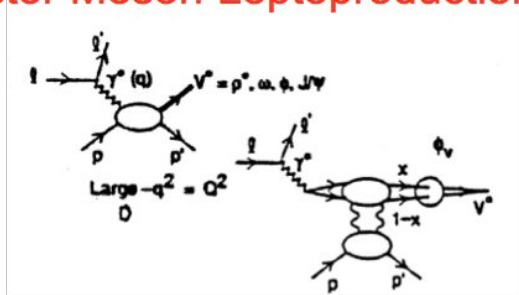
Form Factors $|p \rightarrow l' p'$
 $\langle p' \lambda' | J^+(0) | p \lambda \rangle$



Virtual Compton $\gamma^* p \rightarrow \gamma' p'$
 $\langle p' \lambda' | J^\mu(z) J^\nu(0) | p \lambda \rangle$

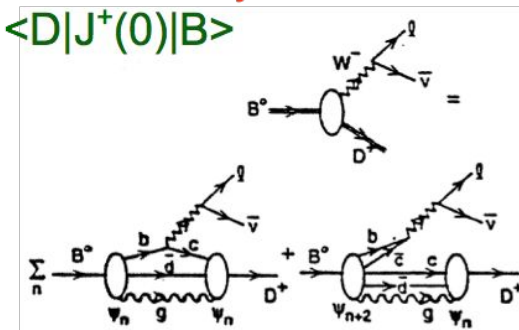


Vector Meson Leptoproduction $\gamma^* p \rightarrow V^* p'$

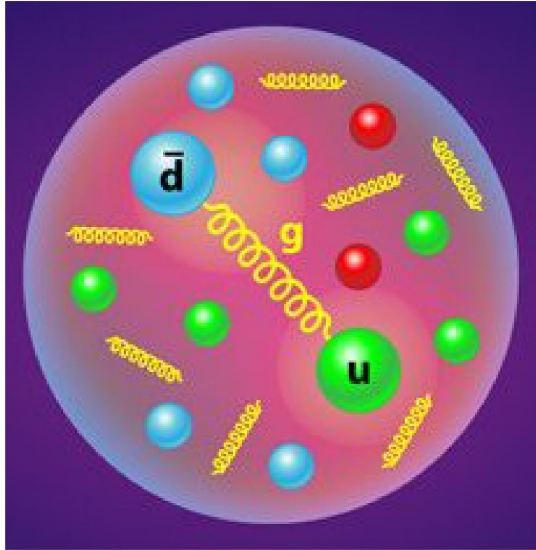


Weak Decay

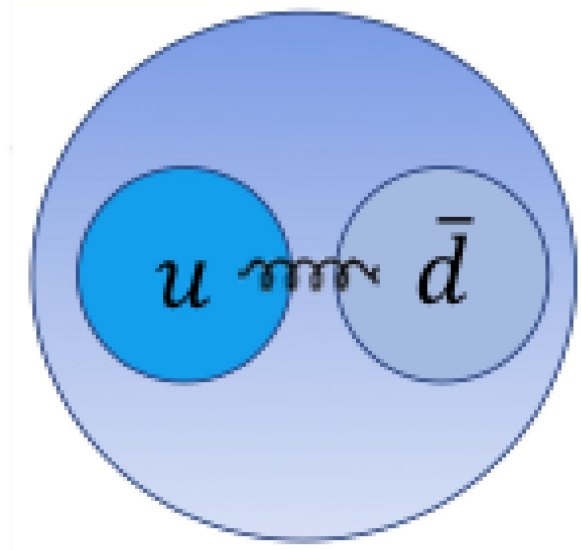
$\langle D | J^+(0) | B \rangle$



Take advantage of LFD and Construct the Light-Front Quark Model (LFQM)



QCD



LFQM

Bakamjian-Thomas Construction in LFD

B. Bakamjian and L. H. Thomas, Phys. Rev. 92, 1300 (1953).

Add interactions to the non-interacting representations without spoiling the Poincare Algebra satisfied by the interacting physical system.

$$M := M_0 + V$$

with

$$[\mathbf{E}_\perp, V]_- = [K^3, V]_- = [\mathbf{j}_{f0}, V]_- = [\mathbf{P}_\perp, V]_- = [P^+, V]_- = 0.$$

Effective Constituent Quark Model for Low Q^2

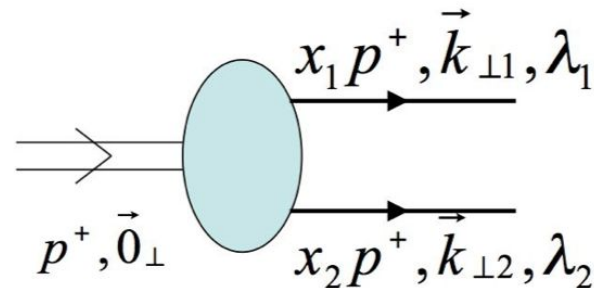
$$|Meson\rangle = \psi_{q\bar{q}}|q\bar{q}\rangle + \psi_{q\bar{q}g}|q\bar{q}g\rangle + \dots$$

$$\approx \Psi_{Q\bar{Q}}|Q\bar{Q}\rangle,$$

where

$$|Q\rangle = \psi_q^Q|q\rangle + \psi_{qg}^Q|qg\rangle + \dots$$

$$|\bar{Q}\rangle = \psi_{\bar{q}}^{\bar{Q}}|\bar{q}\rangle + \psi_{\bar{q}g}^{\bar{Q}}|\bar{q}g\rangle + \dots$$



$$\Psi_{Q\bar{Q}}(x_i, \vec{k}_{\perp i}, \lambda_i) = \Phi(x_i, \vec{k}_{\perp i}) \chi(x_i, \vec{k}_{\perp i}, \lambda_i)$$

Radial

(Dependent on the model potential)

$$H = T + V$$

V includes Coulomb, Confinement,
Spin-Spin, Spin-Orbit interactions.

Spin-Orbit

(Interaction independent Melosh transformation)

$$J^{PC} = 0^{++}(f_0, a_0, \dots)$$

$$0^{-+}(\pi, K, \eta, \eta', \dots)$$

$$1^{-}(\rho, K^*, \omega, \phi, \dots)$$

...

PHYSICAL REVIEW C **92**, 055203 (2015)

Variational analysis of mass spectra and decay constants ...

Ho-Meoyng Choi,¹ Chueng-Ryong Ji,² Ziyue Li,² and Hui-Young Ryu¹

¹*Department of Physics, Teachers College, Kyungpook National University, Daegu, Korea 702-701*

²*Department of Physics, North Carolina State University, Raleigh, North Carolina 27695-8202, USA*

(Received 15 September 2015; published 13 November 2015)

$(\overline{9657}) \eta_b(\overline{9389}) \underline{9407}_{+19}^{-18}$	$(\overline{9691}) \Upsilon(\overline{9460}) \underline{9434}_{-9}^{-6}$
$(\overline{6459}) B_c(\overline{6277}) \underline{6301}_{+14}^{-12}$	$(\overline{6494}) B_c^*(?) \underline{6330}_{-5}^{-3}$
$(\overline{5375}) B_s(\overline{5366}) \underline{(5314)}$	$(\overline{5424}) B_s^*(\overline{5415})(\underline{5333})$
$(\overline{5235}) B(\overline{5279}) \underline{(5233)}$	$(\overline{5315}) B^*(\overline{5325}) \underline{(5268)}$
$(\overline{3171}) \eta_c(\overline{2980}) \underline{3055}_{+25}^{-18}$	$(\overline{3225}) J/\psi(\overline{3097}) \underline{3102}_{-8}^{-4}$
$(\overline{2011}) D_s(\overline{1968})(\underline{1981})$	$(\overline{2109}) D_s^*(\overline{2112})(\underline{2031})$
$(\overline{1836}) D(\overline{1870}) \underline{(1875)}$	$(\overline{1998}) D(\overline{2010}) \underline{(1962)}$
$(\overline{958}) \eta'(\overline{958}) \underline{(958)}$	$(\overline{850}) \underline{(1020)} \phi(\overline{1020}) \underline{(1020)} \underline{(835)}$
$(\overline{548}) \eta(\overline{548}) \underline{(548)}$	$(\overline{782}) \underline{(770)} \rho(\overline{775}) \underline{(780)} \underline{(782)}$
$(\overline{478}) K(\overline{494}) \underline{(510)}$	$K^*(\overline{892}) \underline{\omega(782)}$
$(\overline{140}) \pi(\overline{140}) \underline{(140)}$	
CJ Model Exp. This work	CJ Model Exp. This work

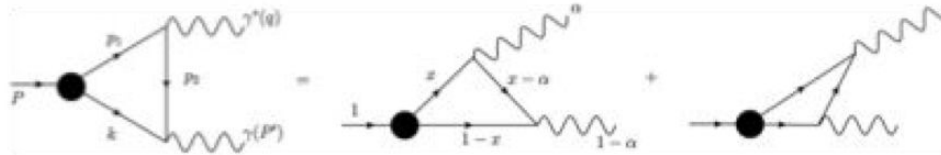
Chiral anomaly and the pion properties in the light-front quark model

Ho-Meoyng Choi

Department of Physics, Teachers College, Kyungpook National University, Daegu 41566, Korea

Chueng-Ryong Ji

Department of Physics, North Carolina State University, Raleigh, North Carolina 27695-8202, USA



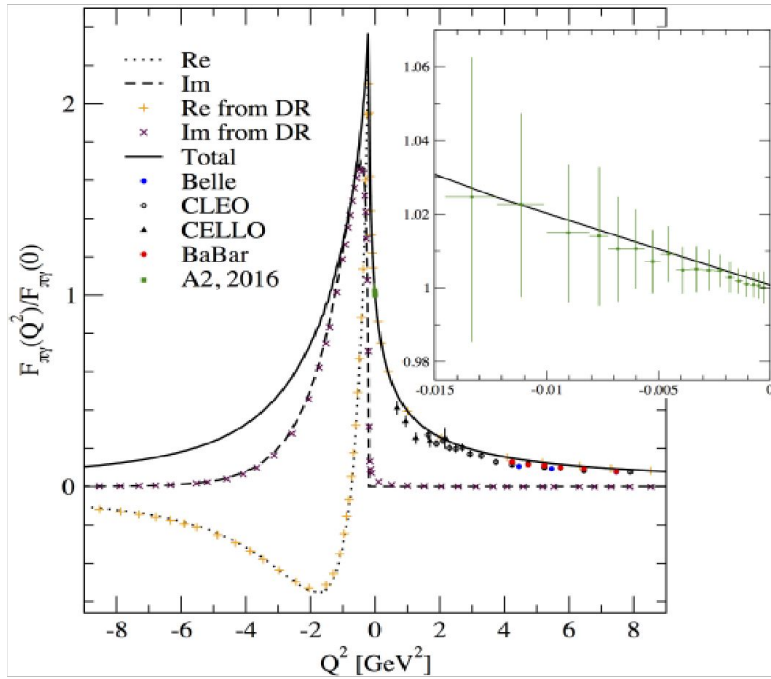
$$\Gamma_{\pi^0 \rightarrow \gamma\gamma} = \frac{\pi}{4} \alpha_{\text{em}}^2 M_\pi^3 |F_{\pi\gamma}(0)|^2$$

$$\Psi_{Q\bar{Q}}^\pi \equiv \Psi_\pi(x_i, \mathbf{k}_{i\perp}, \lambda_i) = \phi_R(x_i, \mathbf{k}_{i\perp}) \chi(x_i, \mathbf{k}_{i\perp}, \lambda_i),$$

$$\chi_{\lambda_1\lambda_2}(x, \mathbf{k}_\perp) = \mathcal{N} \bar{u}_{\lambda_1}(k_1) \Gamma_\pi v_{\lambda_2}(k_2),$$

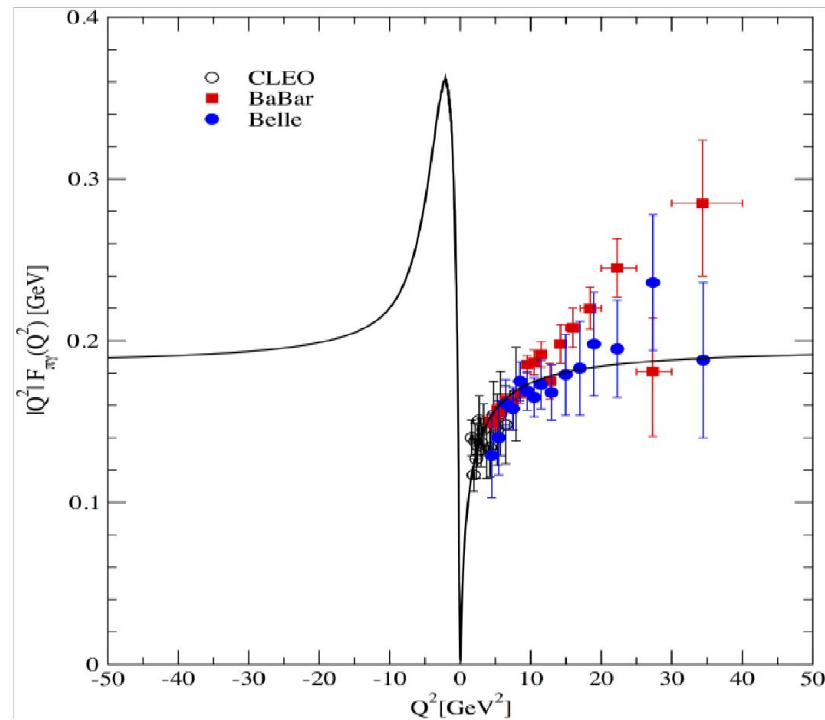
$$\Gamma_\pi = (A_\pi + B_\pi \not{P}) \gamma_5$$

$$F_{\pi\gamma}(q^2) = \frac{e_u^2 - e_d^2}{\sqrt{2}} \frac{\sqrt{2N_c}}{4\pi^3} \int_0^1 \frac{dx}{(1-x)} \int d^2\mathbf{k}_\perp \frac{\psi_\pi(x, \mathbf{k}_\perp)}{M_0^2 - q^2}$$



Both spacelike and timelike form factors can be computed in LFQM.

H.-M. Choi, H.-Y. Ryu, C.-R. Ji,
PRD96, 056008 (2017)



Can IFD and LFD be linked?

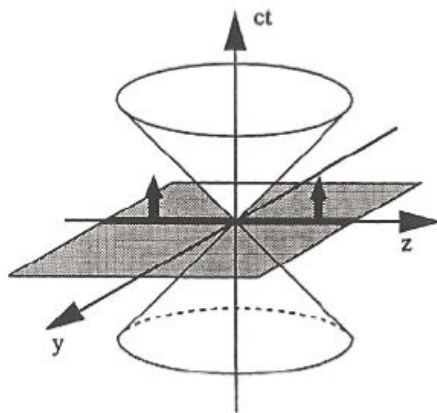


1949

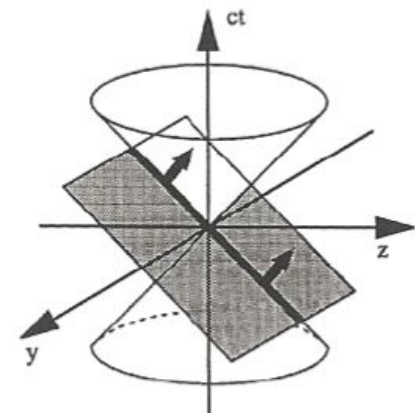


Yes, they can!

1992~2021



The instant form



The front form

Traditional approach
evolved from NR dynamics

Close contact with
Euclidean space

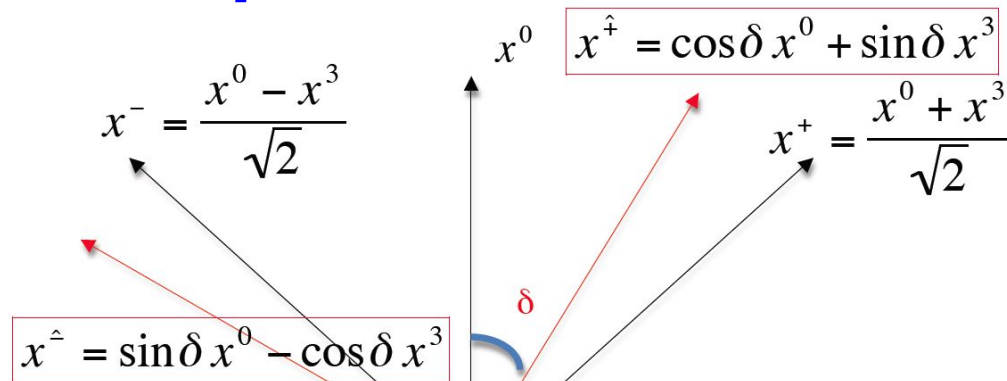
T-dept QFT, LQCD, IMF, etc.

Innovative approach
for relativistic dynamics

Strictly in Minkowski space

DIS, PDFs, DVCS, GPDs, etc.

Interpolation between IFD and LFD



K. Hornbostel, PRD45, 3781 (1992) – RQFT

C.Ji and S.Rey, PRD53, 5815 (1996) – Chiral Anomaly

C.Ji and C. Mitchell, PRD64, 085013 (2001) – Poincare Algebra

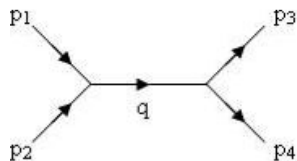
C.Ji and A. Suzuki, PRD87, 065015 (2013) – Scattering Amps

C.Ji, Z. Li and A. Suzuki, PRD91, 065020 (2015) – EM Gauges

Z.Li, M. An and C.Ji, PRD92, 105014 (2015) – Spinors

C.Ji, Z.Li, B.Ma and A.Suzuki, PRD98, 036017 (2018) – QED

B.Ma and C.Ji, PRD104, 036004 (2021), – QCD₁₊₁



$$\delta = 0$$

$$p_0 = p^0$$

$$-p_3 = p^3$$

$$0 < \delta < \pi/4$$

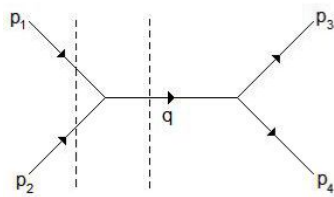
$$p_{\hat{+}} = p^0 \cos \delta - p^3 \sin \delta$$

$$p_{\hat{-}} = p^0 \sin \delta + p^3 \cos \delta$$

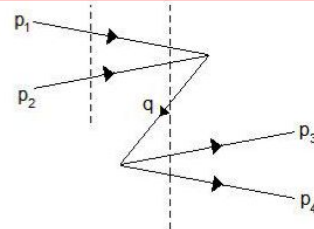
$$\delta = \pi/4$$

$$p_+ = p^-$$

$$p_- = p^+$$



(a)



(b)

$$\frac{1}{2q^0} \left(\frac{1}{p_1^0 + p_2^0 - q^0} - \frac{1}{p_1^0 + p_2^0 + q^0} \right)$$

$$\frac{1}{2\omega_q} \left(\frac{1}{P_{\hat{+}} + \frac{\mathbb{S}q_- - \omega_q}{\mathbb{C}}} - \frac{1}{P_{\hat{+}} + \frac{\mathbb{S}q_- + \omega_q}{\mathbb{C}}} \right)$$

$$\frac{1}{P^+} \left\{ P^- - \frac{(\vec{P}_1^2 + m^2)}{2P^+} \right\}$$

$$\omega_q = \sqrt{q_-^2 + \mathbb{C}(\vec{q}_1^2 + m^2)}$$

$$\mathbb{C} = \cos 2\delta$$

$$\mathbb{S} = \sin 2\delta$$

$$\frac{\mathbb{S}q_- + \omega_q}{\mathbb{C}} \rightarrow \frac{2}{\mathbb{C}} - \frac{\vec{q}_1^2 + m^2}{2q_-} + \mathcal{O}(\mathbb{C})$$

$$\rightarrow \infty \text{ as } \mathbb{C} \rightarrow 0$$

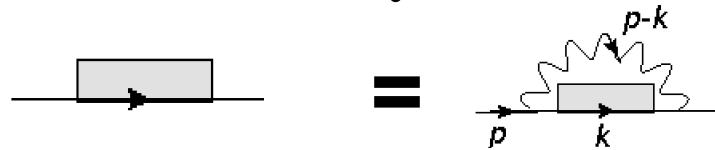
Large N_c QCD in 1+1 dim. ('tHooft Model)

Interpolating 't Hooft model between instant and front forms

Bailing Ma and Chueng-Ryong Ji

PRD104, 036004(2021)

MASS GAP EQUATION



$$\text{---} + \text{---} + \text{---} + \text{---} + \dots \equiv \text{---} \equiv i \Sigma(p)$$

$$\Sigma(p_{\hat{-}}) = i \frac{\lambda}{2\pi} \int \frac{dk_{\hat{-}} dk_{\hat{+}}}{(p_{\hat{-}} - k_{\hat{-}})^2} \gamma^{\hat{+}} \frac{1}{\not{k} - m - \Sigma(k_{\hat{-}}) + i\epsilon} \gamma^{\hat{+}}$$

Fermion Propagator

Free Propagator

$$S_f(p) = \frac{1}{\not{p} - m + i\epsilon}$$



Interacting Propagator

$$S(p) = \frac{1}{\not{p} - m - \Sigma(p) + i\epsilon}$$
$$= \frac{F(p)}{\not{p} - M(p) + i\epsilon}$$

$$\Sigma(p) = \Sigma_s(p) + \Sigma_v(p)\not{p}$$

$$F(p) = (1 - \Sigma_v(p))^{-1} \quad \text{“Wave function renormalization factor”}$$

$$M(p) = \frac{m + \Sigma_s(p)}{1 - \Sigma_v(p)} \quad \text{“Renormalized fermion mass function”}$$

Energy-Momentum Dispersion Relation

Free particle

Interacting particle

$$E = \sqrt{p_z^2 + m^2}$$

$$\frac{F(p'_\perp)E(p'_\perp)}{\sqrt{C}} = \sqrt{p'^2_\perp + M(p'_\perp)^2} \equiv \tilde{E}(p'_\perp)$$

$$\theta_f = \tan^{-1}(p_z / m)$$

$$\theta(p'_\perp) = \theta_f(p'_\perp) + 2\zeta(p'_\perp)$$

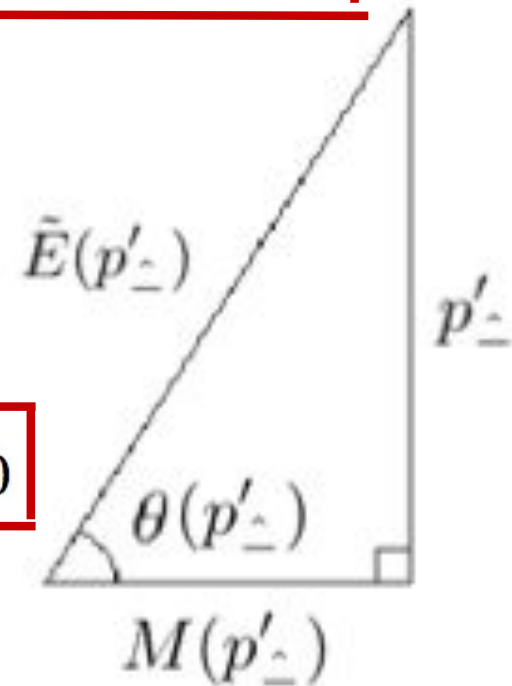
$$\beta = p_z / E$$

$$\begin{pmatrix} b^i(p'_\perp) \\ d^{+i}(p'_\perp) \end{pmatrix} = \begin{pmatrix} \cos\zeta(p'_\perp) & -\sin\zeta(p'_\perp) \\ \sin\zeta(p'_\perp) & \cos\zeta(p'_\perp) \end{pmatrix} \begin{pmatrix} b^i_f(p'_\perp) \\ d^{+i}_f(p'_\perp) \end{pmatrix}$$

$$= \sin\theta_f$$

$$= \tanh\eta$$

$$b^i_f |0\rangle = 0, d^{+i}_f |0\rangle = 0 \text{ vs. } b^i |\Omega\rangle = 0, d^{+i} |\Omega\rangle = 0$$



Interpolation

$$(E, p_z) \Rightarrow (p^\dagger / \sqrt{C}, p_\perp / \sqrt{C} \equiv p'_\perp)$$

Mass Gap Equation in Scaled Variables

$$\bar{p}'_{\hat{z}} = \frac{\bar{p}_{\hat{z}}}{\sqrt{\mathbb{C}}}, \quad \bar{E}' = \frac{\bar{E}}{\sqrt{\mathbb{C}}}, \quad \bar{p}_{\hat{z}} = \frac{p_{\hat{z}}}{\sqrt{2\lambda}}, \quad \bar{E} = \frac{E}{\sqrt{2\lambda}}, \quad \bar{m} = \frac{m}{\sqrt{2\lambda}}$$

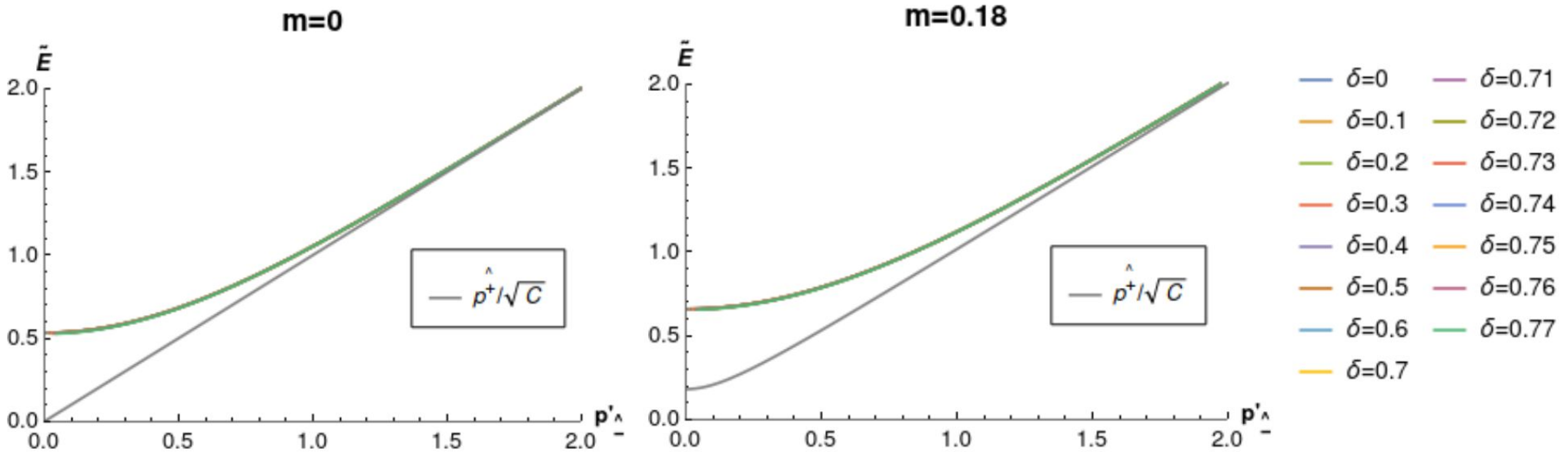
$$\bar{p}'_{\hat{z}} \cos \theta(\bar{p}'_{\hat{z}}) - \bar{m} \sin \theta(\bar{p}'_{\hat{z}}) = \frac{1}{4} \int \frac{d\bar{k}'_{\hat{z}}}{(\bar{p}'_{\hat{z}} - \bar{k}'_{\hat{z}})^2} \sin \left(\theta(\bar{p}'_{\hat{z}}) - \theta(\bar{k}'_{\hat{z}}) \right)$$

$$\bar{E}'(\bar{p}'_{\hat{z}}) = \bar{p}'_{\hat{z}} \sin \theta(\bar{p}'_{\hat{z}}) + \bar{m} \cos \theta(\bar{p}'_{\hat{z}}) + \frac{1}{4} \int \frac{d\bar{k}'_{\hat{z}}}{(\bar{p}'_{\hat{z}} - \bar{k}'_{\hat{z}})^2} \cos \left(\theta(\bar{p}'_{\hat{z}}) - \theta(\bar{k}'_{\hat{z}}) \right)$$

$$\frac{p_{\hat{z}}}{\mathbb{C}} \cos \theta(p_{\hat{z}}) - \frac{m}{\sqrt{\mathbb{C}}} \sin \theta(p_{\hat{z}}) = \frac{\lambda}{2} \int \frac{dk_{\hat{z}}}{(p_{\hat{z}} - k_{\hat{z}})^2} \sin \left(\theta(p_{\hat{z}}) - \theta(k_{\hat{z}}) \right)$$

$$E(p_{\hat{z}}) = p_{\hat{z}} \sin \theta(p_{\hat{z}}) + \sqrt{\mathbb{C}} m \cos \theta(p_{\hat{z}}) + \frac{\mathbb{C}\lambda}{2} \int \frac{dk_{\hat{z}}}{(p_{\hat{z}} - k_{\hat{z}})^2} \cos \left(\theta(p_{\hat{z}}) - \theta(k_{\hat{z}}) \right)$$

Mass Gap Solutions



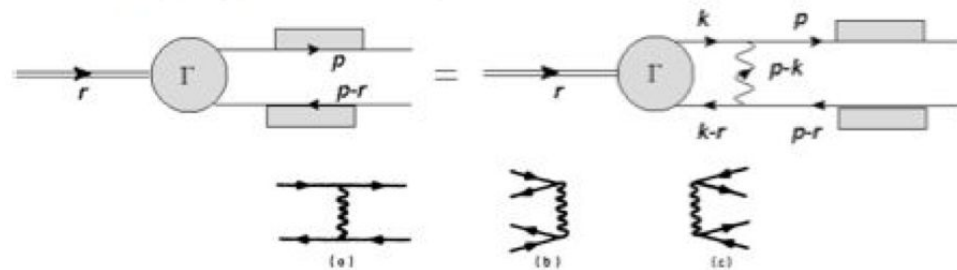
$$\tilde{E}(0) = \frac{F(0)E(0)}{\sqrt{C}} = M(0)$$

m	0	0.045	0.18	0.749	1.00	2.11	4.23
$M(0)$	0.532778	0.563644	0.659112	1.10105	1.31167	2.30969	4.34358
$F(0)$	-0.495173	-0.584175	-0.987673	4.11079	2.17976	1.22134	1.05526

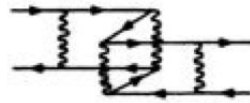
$$m \lesssim 0.56$$

BOUND-STATE EQUATION

$$\Gamma(r, p) = \frac{i\lambda}{2\pi} \int \frac{dk_{\perp} dk_{\parallel}}{(p_{\perp} - k_{\perp})^2} S(p) \gamma^{\dagger} \Gamma(r, k) \gamma^{\dagger} S(p - r)$$



$$\begin{aligned} & \left[-r_{\parallel} + \frac{-Sp_{\perp} + E(p_{\perp})}{C} + \frac{S(p_{\perp} - r_{\perp}) + E(p_{\perp} - r_{\perp})}{C} \right] \hat{\phi}_{+}(r_{\perp}, p_{\perp}) \\ &= \lambda \int \frac{dk_{\perp}}{(p_{\perp} - k_{\perp})^2} \left[C(p_{\perp}, k_{\perp}, r_{\perp}) \hat{\phi}_{+}(r_{\perp}, k_{\perp}) - S(p_{\perp}, k_{\perp}, r_{\perp}) \hat{\phi}_{-}(r_{\perp}, k_{\perp}) \right], \\ & \left[r_{\parallel} + \frac{-S(p_{\perp} - r_{\perp}) + E(p_{\perp} - r_{\perp})}{C} + \frac{Sp_{\perp} + E(p_{\perp})}{C} \right] \hat{\phi}_{-}(r_{\perp}, p_{\perp}) \\ &= \lambda \int \frac{dk_{\perp}}{(p_{\perp} - k_{\perp})^2} \left[C(p_{\perp}, k_{\perp}, r_{\perp}) \hat{\phi}_{-}(r_{\perp}, k_{\perp}) - S(p_{\perp}, k_{\perp}, r_{\perp}) \hat{\phi}_{+}(r_{\perp}, k_{\perp}) \right]. \end{aligned}$$



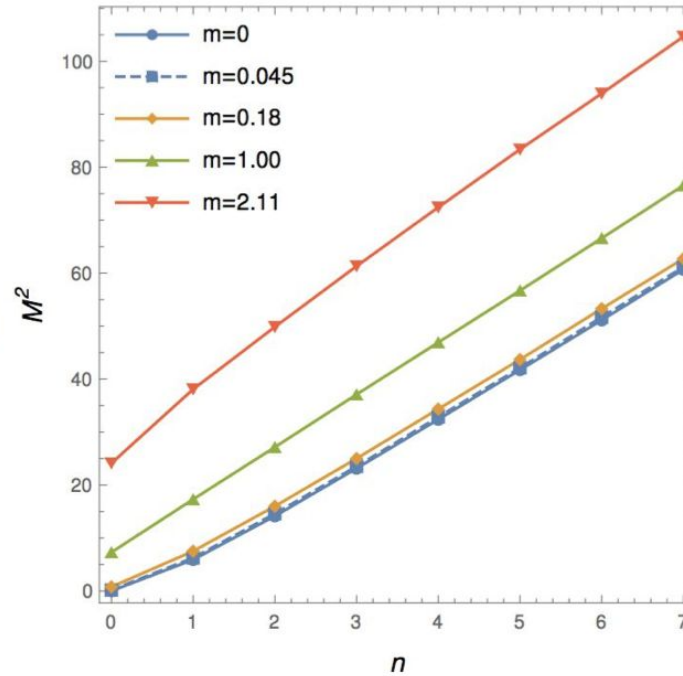
LFD

$$\left[\mathcal{M}^2 - \frac{m^2 - 2\lambda}{x} - \frac{m^2 - 2\lambda}{1-x} \right] \phi(x) = -2\lambda \int_0^1 \frac{dy}{(x-y)^2} \phi(y)$$

Meson Spectroscopy

LFD

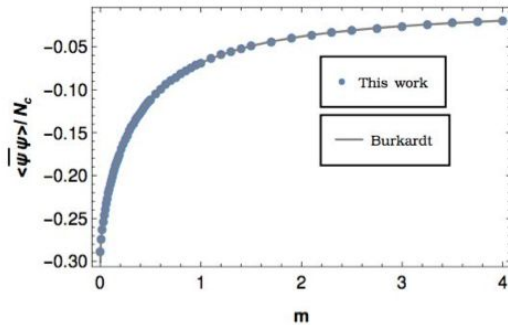
**G.'tHooft,
NPB75,461
(1974)**



IFD

**Li,Wilets,Birse
JPG:NP13,915
(1987)**

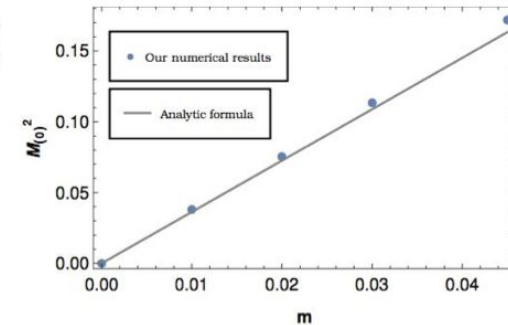
**Jia,Liang,Xiong
JHEP11,151
(2017)**



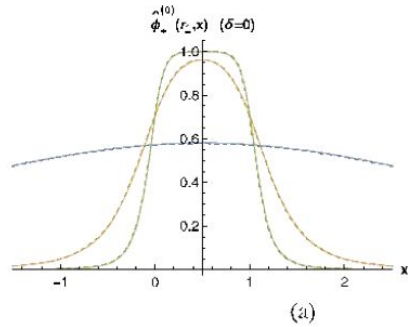
$$\mathcal{M}_\pi^2 = -\frac{4m \langle \bar{\psi}\psi \rangle}{f_\pi^2} = \sqrt{\frac{8\pi^2 m^2 \lambda}{3}}$$

$$f_\pi = \sqrt{N_c/\pi}$$

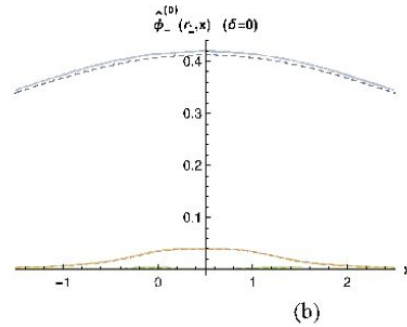
$$\langle \bar{\psi}\psi \rangle = -N_c/\sqrt{12}$$



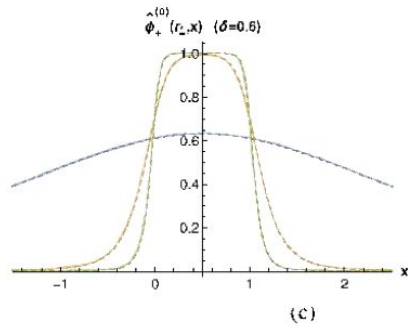
Meson Wavefunctions



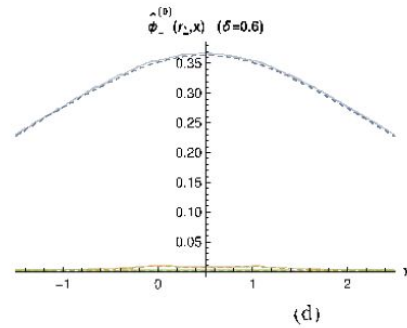
- $r_- = 0.2 M_{0,16}$, analytic
- $r_- = 2 M_{0,8}$, analytic
- $r_- = 5 M_{0,8}$, analytic
- - - $r_- = 0.2 M_{0,18}$
- - - $r_- = 2 M_{0,18}$
- - - $r_- = 5 M_{0,18}$



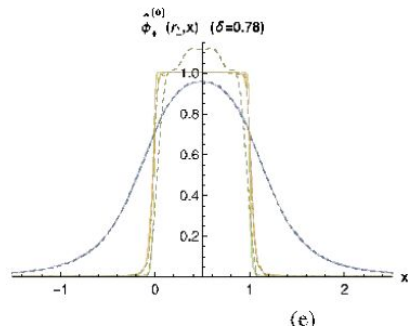
- $r_- = 0.2 M_{0,18}$, analytic
- $r_- = 2 M_{0,18}$, analytic
- $r_- = 5 M_{0,18}$, analytic
- - - $r_- = 0.2 M_{0,18}$
- - - $r_- = 2 M_{0,18}$
- - - $r_- = 5 M_{0,18}$



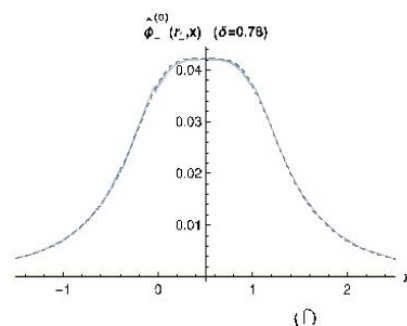
- $r_- = 0.2 M_{0,16}$, analytic
- $r_- = 2 M_{0,8}$, analytic
- $r_- = 5 M_{0,8}$, analytic
- - - $r_- = 0.2 M_{0,18}$
- - - $r_- = 2 M_{0,18}$
- - - $r_- = 5 M_{0,18}$



- $r_- = 0.2 M_{0,18}$, analytic
- $r_- = 2 M_{0,18}$, analytic
- $r_- = 5 M_{0,18}$, analytic
- - - $r_- = 0.2 M_{0,18}$
- - - $r_- = 2 M_{0,18}$
- - - $r_- = 5 M_{0,18}$



- $r_- = 0.2 M_{0,16}$, analytic
- $r_- = 2 M_{0,8}$, analytic
- $r_- = 5 M_{0,8}$, analytic
- - - $r_- = 0.2 M_{0,18}$
- - - $r_- = 2 M_{0,18}$
- - - $r_- = 5 M_{0,18}$



- $r_- = 0.2 M_{0,18}$, analytic
- $r_- = 2 M_{0,18}$, analytic
- $r_- = 5 M_{0,18}$, analytic
- - - $r_- = 0.2 M_{0,18}$
- - - $r_- = 2 M_{0,18}$
- - - $r_- = 5 M_{0,18}$

Parton Distribution Functions (PDFs)

$$q_n(x) = \int_{-\infty}^{+\infty} \frac{d\xi^-}{4\pi} e^{-ixP^+\xi^-} \\ \times \langle P_n^-, P^+ | \bar{\psi}(\xi^-) \gamma^+ \mathcal{W}[\xi^-, 0] \psi(0) | P_n^-, P^+ \rangle_C,$$

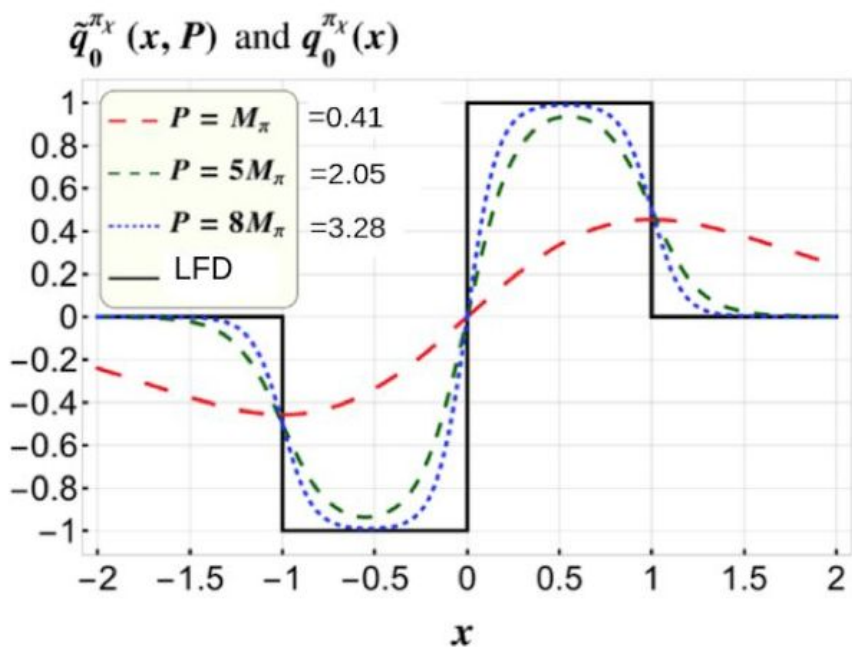
$$\mathcal{W}[\xi^-, 0] = \mathcal{P} \left[\exp \left(-ig_s \int_0^{\xi^-} d\eta^- A^+(\eta^-) \right) \right] \mathbf{A^+=0 Gauge} \\ \mathbf{in LFD}$$

Quasi-PDFs

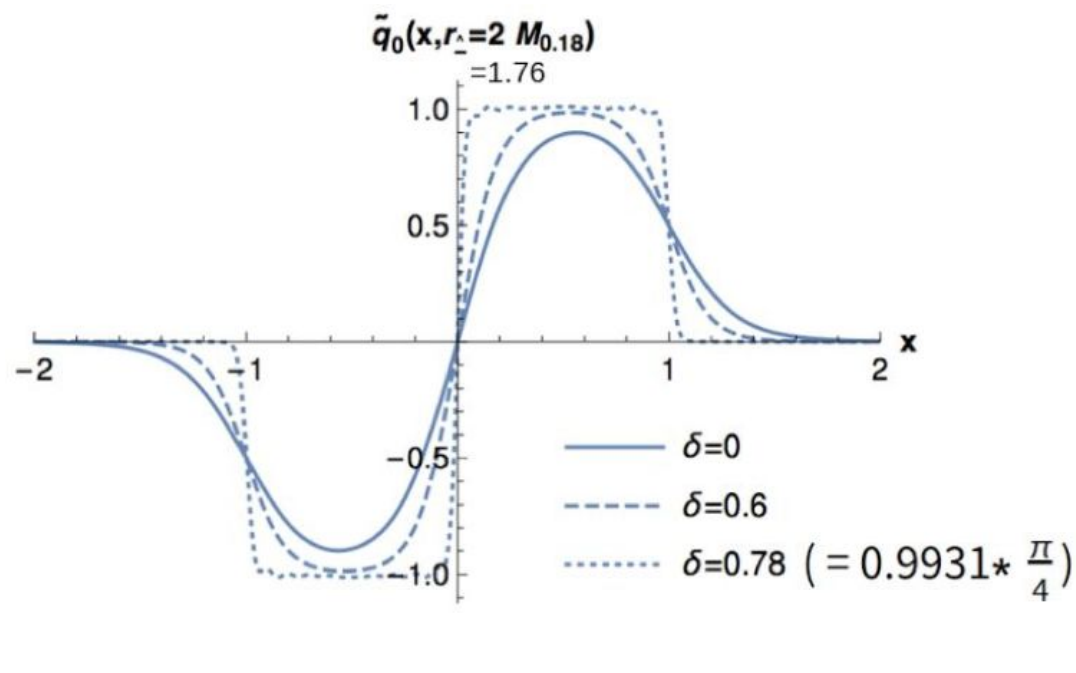
$$\tilde{q}_{(n)}(r_\perp, x) = \int_{-\infty}^{+\infty} \frac{dx^\perp}{4\pi} e^{ix^\perp r_\perp} \\ \times \langle r_{(n)}^\perp, r_\perp | \bar{\psi}(x^\perp) \gamma_\perp \mathcal{W}[x^\perp, 0] \psi(0) | r_{(n)}^\perp, r_\perp \rangle_C,$$

$$\mathcal{W}[x^\perp, 0] = \mathcal{P} \left[\exp \left(-ig \int_0^{x^\perp} dx'^\perp A_\perp(x'^\perp) \right) \right] \mathbf{Interpolating} \\ \mathbf{dynamics}$$

Quasi-PDF



Quark quasi-PDFs and light-front PDF for the chiral pion.



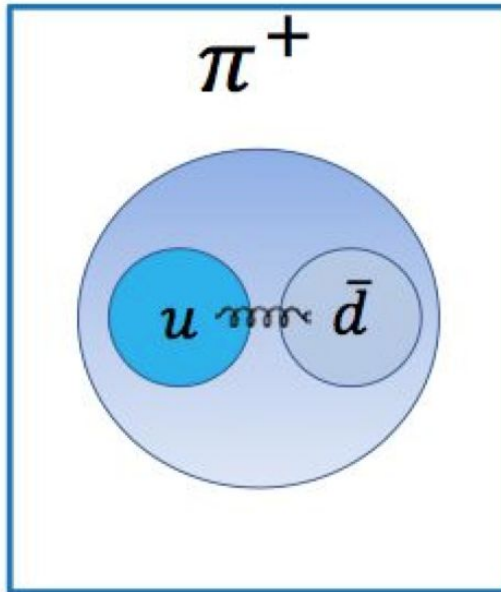
Interpolating "quasi-PDFs" for the chiral pion.

All quantities are in proper units of $\sqrt{2\lambda}$.

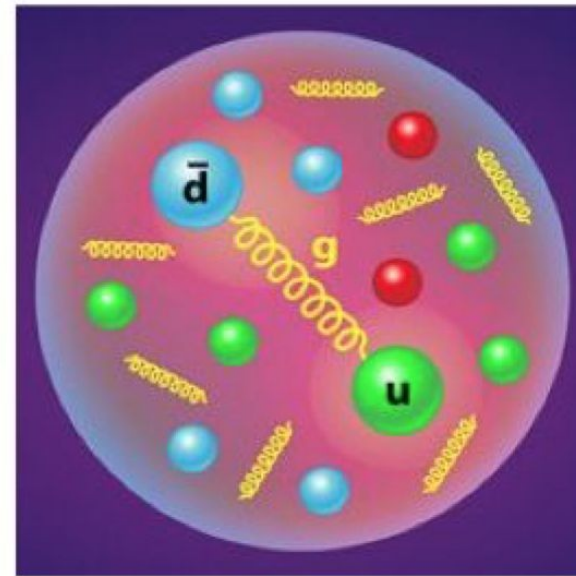
Jia, Y., Liang, S., Xiong, X., and Yu, R. (2018). Phys. Rev. D, 98:054011.

Ma, B. and Ji, C.-R. (2021). Phys. Rev. D, 104:036004.

Pion's Dichotomy



vs.



Constituent Quark Model

$$M = m_1 + m_2 + A \frac{\vec{s}_1 \cdot \vec{s}_2}{m_1 m_2}$$

$$m_u = m_d = 310 \text{ MeV} / c^2$$

$$A = \left(\frac{2m_u}{\hbar} \right)^2 160 \text{ MeV} / c^2$$

Quantum Chromodynamics

Isospin symmetry

Chiral symmetry

$SU(2)_R \times SU(2)_L$

Spontaneous symmetry breakdown

Goldstone Bosons


$$F_\pi^2 M_\pi^2 = -(m_u + m_d) \langle 0 | \bar{u}u | 0 \rangle$$

Effective field theory


Pion Properties

- Lightest bound state composed of quarks, antiquarks, and gluons
- Masses: $m_{\pi^{\pm}} = 139.57 \text{ MeV}$, $m_{\pi^0} = 134.977 \text{ MeV}$
- Lifetimes: $\tau_{\pi^{\pm}} = 2.603 \times 10^{-8} \text{ s}$, $\tau_{\pi^0} = 8.52 \times 10^{-17} \text{ s}$

Charged pions decay via weak interaction

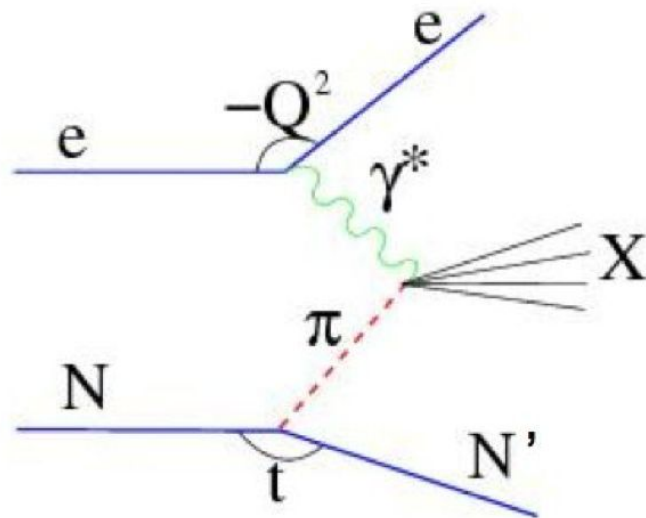


Neutral pions decay via electromagnetic interaction, *i.e.* $\pi^0 \rightarrow \gamma\gamma$



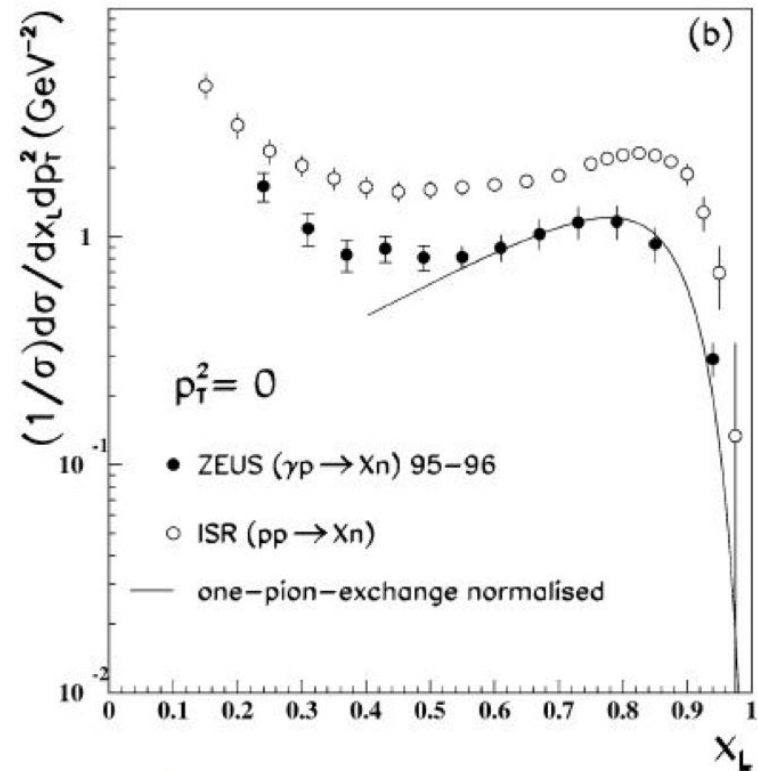
Measurement of Tagged Deep Inelastic Scattering (TDIS)

C.Keppel (Contact person)



$$e + p(\text{or } n) \rightarrow e' + p + X$$

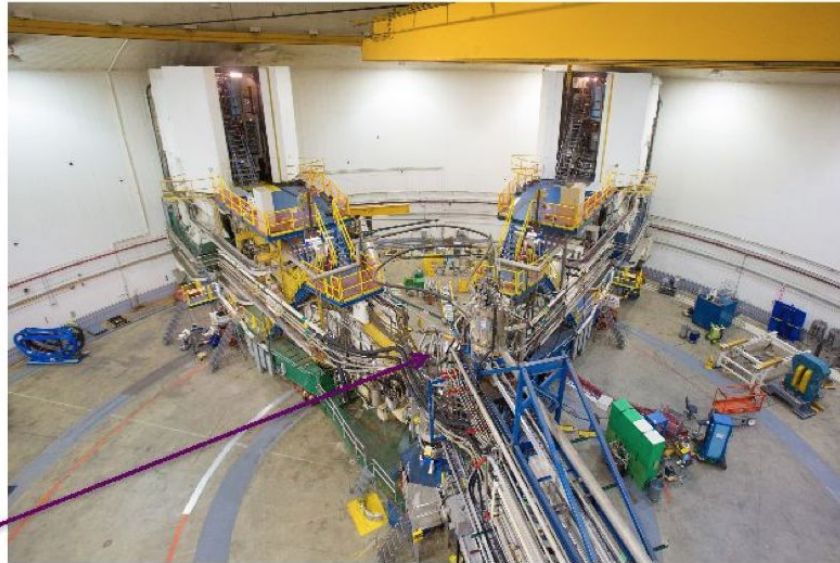
$$e + D \rightarrow e' + p + p + X$$



Leading neutron production in e^+p collisions at HERA

ZEUS Collaboration, NPB 637 (2002) 3–56

JLab Hall A TDIS Experiment

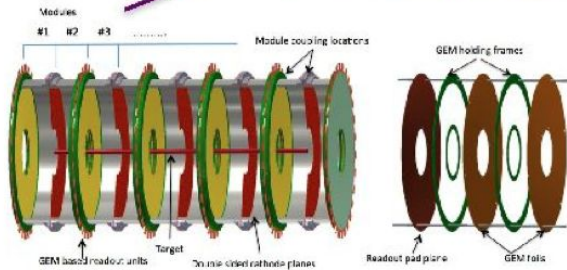


proton tag
detection in
GEM-based
mTPC at pivot

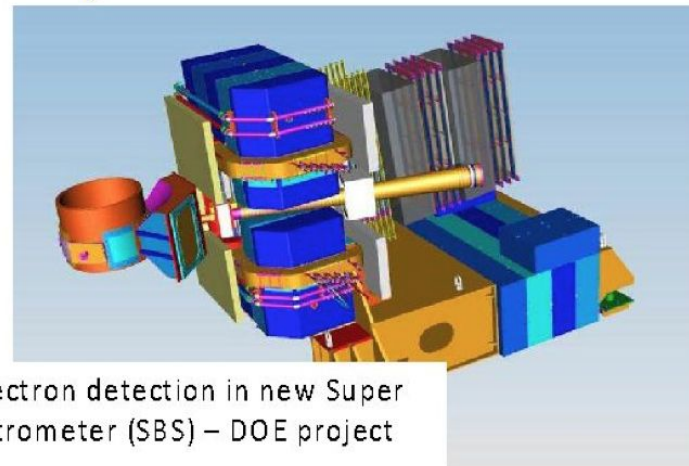
Hall A with SBS:

- High luminosity,
50 μ Amp,
 $L = 3 \times 10^{36} / \text{cm}^2 \text{s}$
 - Large acceptance
 $\sim 70 \text{ msr}$
- Important for small
cross sections**

e- beam

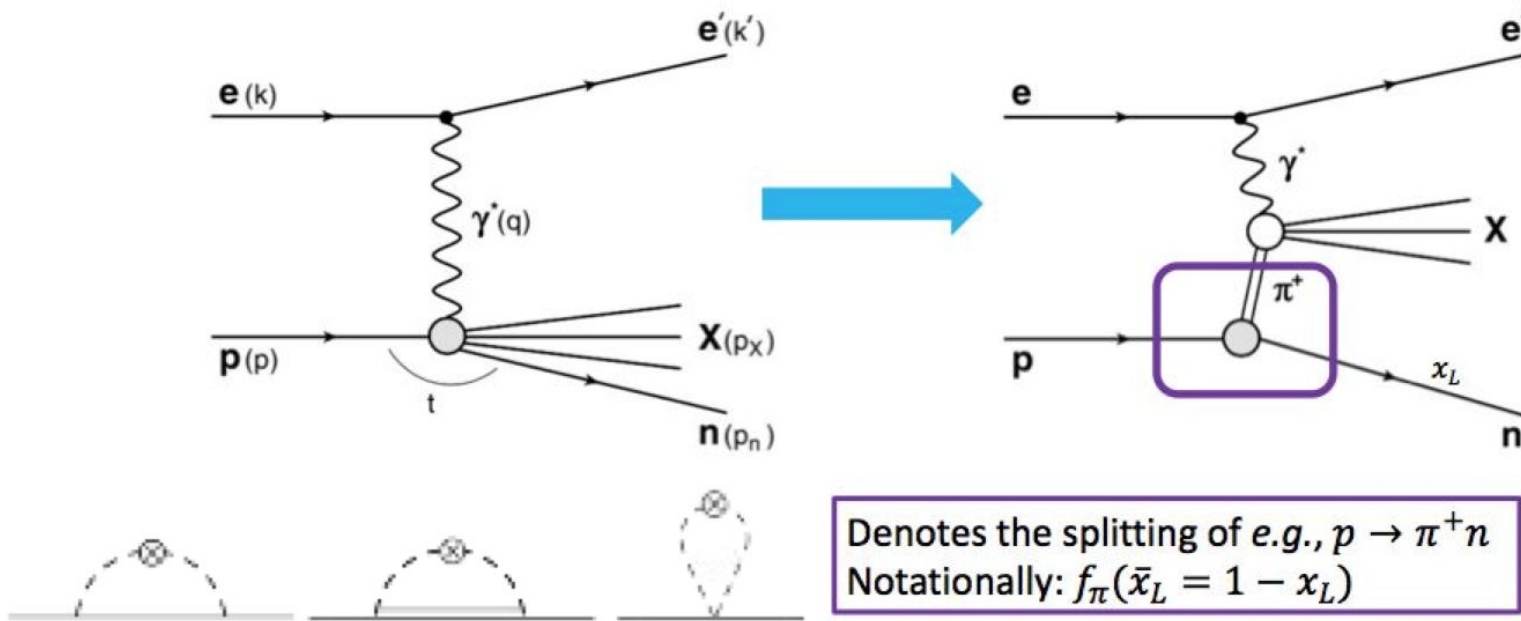


mTPC inside
superconducting
solenoid



Scattered electron detection in new Super
Bigbite Spectrometer (SBS) – DOE project
complete

Convolution with Chiral Effective Theory



$$(\bar{d} - \bar{u})(x) = \frac{2}{3} \int_x^1 \frac{dy}{y} f_\pi(y) \bar{q}^\pi(x/y)$$

pion light-cone momentum distribution in nucleon

First global Monte Carlo analysis of pion PDFs

P. Barry, N. Sato, W. Melnitchouk, C.Ji

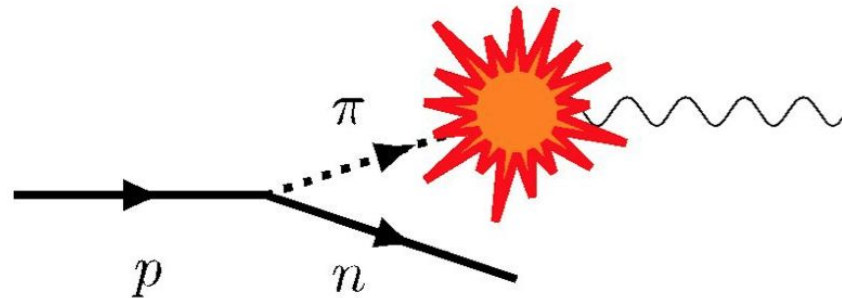
PRL121,152001(2018) Featured in Physics

■ How to probe pion structure

+ $\pi + A \rightarrow l\bar{l} + X$ (Drell-Yan)

+ $\pi + A \rightarrow \gamma + X$ (prompt photons)

+ $e + p \rightarrow e' + n + X$ (SIDIS) \rightarrow small x_π gluon PDF



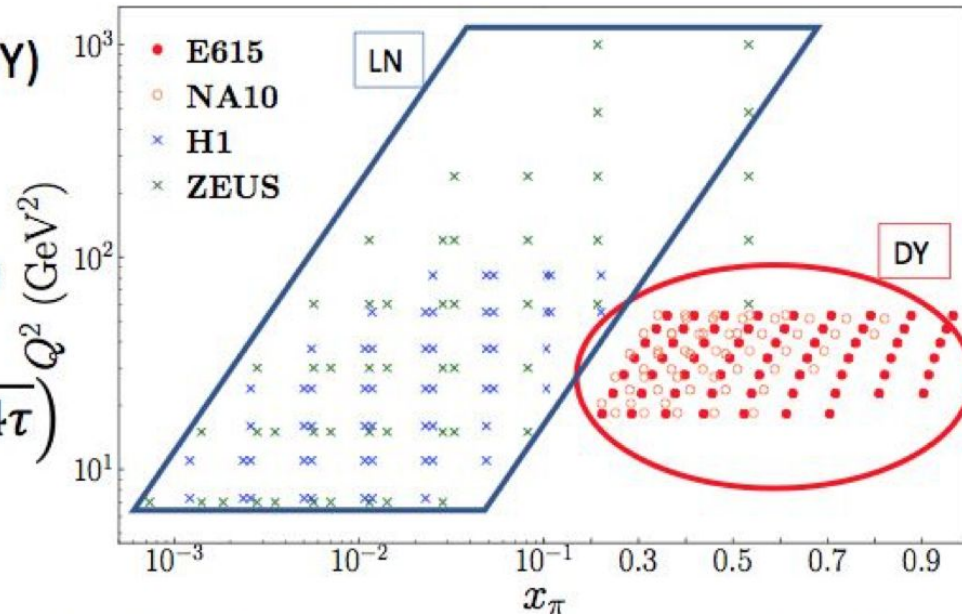
Datasets vs. Kinematics

- Large x_π -- Drell-Yan (DY)
- Small x_π -- Leading Neutron (LN)
- Not much data overlap
- In DY:

$$x_\pi = \frac{1}{2} \left(x_F + \sqrt{x_F^2 + 4\tau} \right)$$

- In LN:

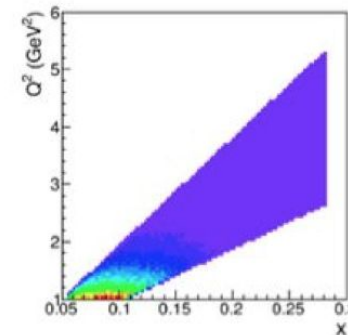
$$x_\pi = x_B / \bar{x}_L$$

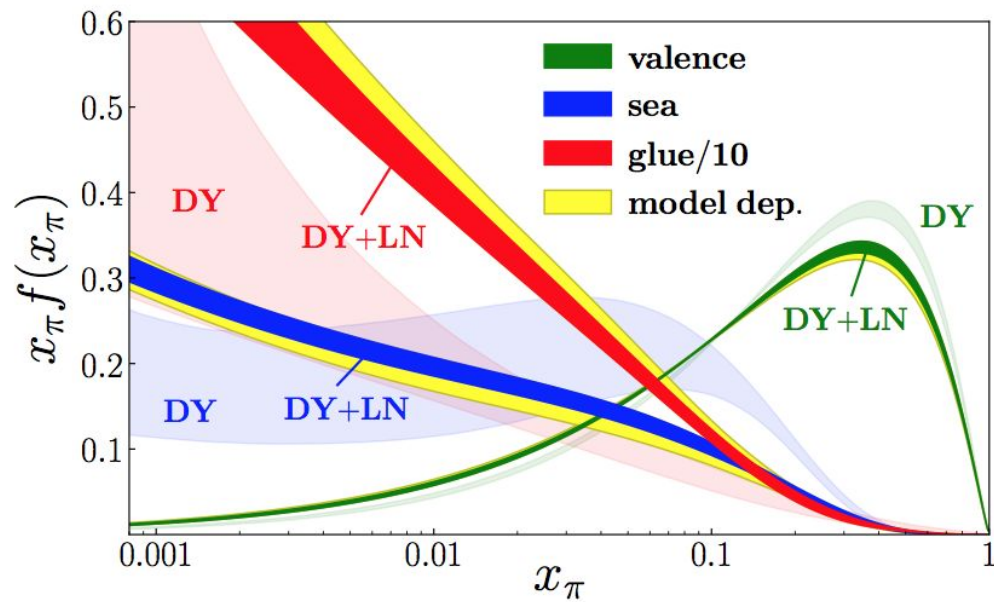


- JLab can reach much smaller Q^2 and larger x range than in the HERA

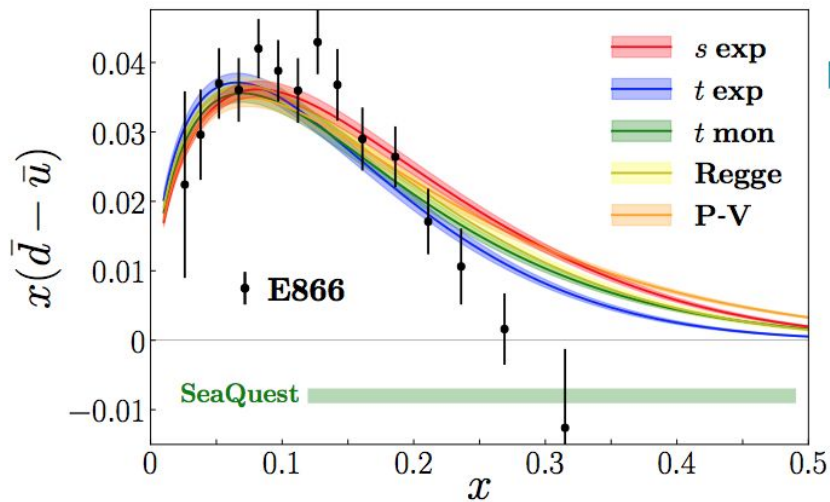
EIC Impact on Pion PDFs

- $s = 5400 \text{ GeV}^2$, 1.2% systematic uncertainty, integrated $\mathcal{L} = 100\text{fb}^{-1}$

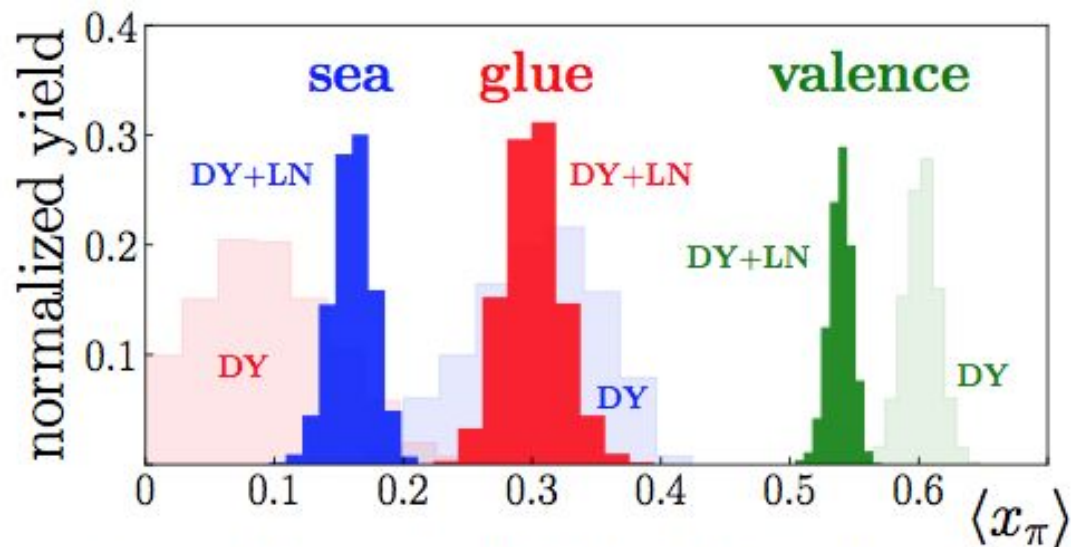




- Significant reduction of the uncertainties
- Non-overlapping uncertainties → tensions among the data
- Accuracy will be improved with future TDIS (JLab12/EIC)



- We performed an additional analysis of LN+DY+E866 → good description of E866 data except for large x



- Constraints from HERA significantly increase $\langle x_\pi^g \rangle$.

The role of the glue is more important than suggested by DY alone

- In contrast, the strength of the sea is reduced
- Due to momentum sum rule $\langle x_\pi^{\text{valence}} \rangle$ decreases

Outlook

- LFD provides a useful tool to study highly nontrivial quantum chromodynamic phenomenology taking advantage its distinguished features such as the boost invariance and the cleaner vacuum properties.
- Corresponding the LFD results with the IFD and its IMF approach is useful to understand the complicated confinement mechanism and the chiral symmetry aspects of QCD and the associated hadron phenomenology.
- Vigorous experimental measurements, e.g. 12 GeV upgrade of Jefferson Lab, future Electron Ion Collider projects, etc. are encouraging to provide deeper understanding on the nature of hadrons.